

Wednesday, September 28, 2005

Teaching Lectures

162

Treatment marginsA. McKenzie*Bristol Oncology Centre, UK*

In addition to recommending standards for prescribing and reporting photon beam therapy, ICRU50 and ICRU62 also recommended that margins be drawn around target volumes and organs at risk in order to account for geometric uncertainty. In particular, these publications introduced the concept of a Planning Target Volume (PTV), produced by drawing treatment margins around the Clinical Target Volume (CTV), and these margins are supposed to be large enough to account for geometric uncertainties.

Errors arising from geometric uncertainties may be divided into (1) systematic errors, represented by a standard deviation Σ , which arise during the preparation for treatment and (2) random errors, represented by a standard deviation σ , resulting from daily differences in set-up and organ motion, if relevant. Sources of systematic error are uncertainties of delineation, phantom transfer (including imaging, treatment planning and transfer to the treatment unit), patient set-up and organ motion. They are systematic because these errors are "frozen" into the treatment delivery, to be repeated on every fraction.

Some geometric uncertainties, such as the linac positioning laser error, the collimator axis error and the collimator edge error, that contribute to the phantom transfer error, are constrained by tolerance limits, generally $\pm 2\text{mm}$. Such uncertainties have a standard deviation of $2/\sqrt{3}$ mm and combine in quadrature. Sources of positional uncertainty do not necessarily have their principal axes aligned with the cardinal patient directions (ant-post, sup-inf and left-right). The general solution is to find the eigenvalues of the sum of the covariance matrices for each of the errors, with principal axes along the eigenvectors, but this may be simplified by expressing the errors always in the cardinal patient directions. Then they may be simply summed in quadrature.

Once the sizes of the combined geometric uncertainties are known, the question is, what size of treatment margin should be drawn around the CTV? Two popular approaches are those of Stroom and colleagues, who advocate margins large enough to ensure that 99% the CTV will receive at least 95% of the prescription dose, and van Herk and colleagues, who suggest margins large enough to ensure that, in 90% of cases, the complete CTV is covered by at least 95% of the prescription dose. These two approaches, while different in philosophy, are both based on criteria that are somewhat arbitrary, and, in fact, result in very similar prescriptions for the margin size ($2.25 \pm 0.25 \Sigma + 0.7\sigma$). Other sources of error, such as breathing, may best be dealt with simply by adding linearly to these margins.

Publication ICRU62 also proposed the addition of margins around Organs at Risk (ORs). For serial-type organs, where damage above a threshold dose to even a very small volume is unacceptable, a margin of 1.3Σ , where Σ is the set-up error, is appropriate if the OR does not change its shape, such as the spinal cord. If the organ changes its shape, a larger margin of 2.5Σ may be more appropriate, where Σ includes the deviation from the mean shape. For parallel-type organs, where it can be acceptable to irradiate a given fraction of the total volume up to a limiting dose, Stroom and colleagues have suggested a different approach that depends upon analysing the effect that such geometric uncertainties will have on the DVHs of irradiated ORs.

Intensity Modulated Radiotherapy (IMRT) adds complexity to the question of treatment margins, but margins are still required, and the same principles that have been used for conformal therapy can still be applied.

163

Dosimetry Protocol in BT (TG-43)M.J. Rivard*Medical Physicist and Brachytherapy Physics, Tufts University School of Medicine**Department of Radiation Oncology, Tufts-New England Medical Center, Boston, Massachusetts, USA*

In 2004, the American Association of Physicists in Medicine (AAPM) published an update (TG-43U1) to the Task Group No. 43 brachytherapy dosimetry protocol (TG-43). The original TG-43 report introduced a new brachytherapy dose calculation formalism in 1995 which was largely based on findings of the ICWG. Previous calculation formalisms were based upon apparent activity, equivalent mass of radium, exposure-rate constants, and tissue-attenuation coefficients. These older formalisms did not account for source-to-source differences in encapsulation or internal construction. With the exception of radium, the exposure-rate constants and other input parameters to these algorithms depended only on the radionuclide. In contrast, TG-43 employed dose-rate constants and other dosimetric parameters that depended on the specific source design, and are directly measured or calculated for each source design. Additionally, TG-43 presented consensus dosimetry data, in terms of the recommended formalism, for the three low-energy (those with average photon energies less than 50 keV) photon-emitting source models then available. These data were based upon a critical review of ICWG-measured dose-rate distributions and Monte Carlo calculations available in the literature. The TG-43 protocol has resulted in significant improvements in the standardization of both dose-calculation methodologies as well as dose-rate distributions used for clinical implementation of brachytherapy, with differences between previously used dose-rate distributions and those now recommended being as large as 17% for some sources. These changes have been reviewed and are generally accepted by the medical physics community and treatment planning software vendors. Approximately 20 new low-energy interstitial brachytherapy source models have been introduced to the market since publication of TG-43. Commercial developments can be attributed to the rising popularity of permanent prostate brachytherapy where some new brachytherapy sources were introduced into practice without thorough scientific evaluation of dosimetric parameters. The AAPM addressed this issue in 1998, recommending that at least one experimental and one Monte Carlo determination of the TG-43 dosimetry parameters be published in the peer-reviewed literature before using new low-energy photon-emitting sources in routine clinical practice. Thus, many source models are supported by multiple dosimetry datasets based upon a variety of basic dosimetry techniques. This confronts the clinical physicist with the problem of critically evaluating and selecting an appropriate dataset for clinical use. To address this problem, this AAPM protocol included a critical review of dosimetry data for twenty ^{125}I and ^{103}Pd source models which satisfied the aforementioned criteria. The present protocol recommends a single, consensus dataset for each source model from which the full 2-D dose-rate distribution can be reconstructed.

164

Dose escalation Radiotherapy Of Prostate CancerA. Widmark*University Hospital, Umea, Sweden*

During the 1990's it became clear that radiotherapy of prostate cancer might benefit from dose escalation. Biopsy data showed that between 20-60% of biopsies 2-3 years after radiotherapy showed remaining cancer like cells. It has also been assumed that local control could influence outcome. However, the largest support for dose escalation was probably the improvement with conformal radiotherapy technique decreasing predominantly rectal toxicity. In the

mid 1990's a number of retrospective comparative analysis from institutional patient series reported improvement in PSA free survival with doses above 70 Gy in comparison to lower doses. Hanks and co-workers published in 1999 a matched pair analysis comparing doses less than 71 Gy with doses above 76 Gy in 714 patients. They showed significant increase in PSA cure rate, metastasis free survival, cancer specific survival and even overall survival at 5 years. Later Pollack and co-workers published the randomised study on 305 patients showing about 25% increase in PSA free survival at 5 years which was also followed by a 5 year increase in metastasis free survival. This was only shown in the patient group with a PSA about 10. Recently Zietman and co-workers showed that dose escalation radiotherapy of patients with low risk prostate cancer also benefited in a similar magnitude as showed in patients with PSA above 10. So far only two studies have been reported results on randomised studies but another 4 studies are waiting to mature.

The obvious risk with dose-escalation radiotherapy is increased rectal and urinary toxicity, which also has been reported in some studies. Others has not been able to show any increase in rectal toxicity after dose escalation radiotherapy. This difference is probably due to the use of different techniques with smaller margins around the prostate. In 1997 we started dose-escalation studies in Umeå using markers with the BeamCath technique, a urethral catheter with implanted fiducial markers. Using prospective comparative evaluation of Quality of Life and Side Effects with the PCSS questionnaire, we have compared side-effects after doses from 64 Gy to 78 Gy. We do not see any significant increase in rectal toxicity at 5 years despite dose-escalation. Over the last years an intense development has occurred to try to visualise or fixate the prostate during radiotherapy treatment. BAT, CT, MRI, implanted markers and balloon fixation are ways to improve radiotherapy treatment of prostate cancer.

Another way of performing further dose escalation radiotherapy of prostate cancer would be to use the recent published suggestions that the α/β value for prostate cancer would be low and this could indicate that HYPO-fractionation would increase the biological effect. Preliminary results from different authors suggest that this is technically feasible. Madison and co-workers have reported their first experience in modern time suggesting that you can give 6.7 Gy x 5 to the prostate. Other centres have also reported on more modest forms of HYPO-fractionation schedules (2.5-3.5 Gy/fraction).

In Scandinavia a large randomised study has recently been started to test this hypothesis by randomising between 2 Gy to 78 Gy Vs 6.1 Gy x 7. Initial preliminary data was reported at ASTRO last year showed that no dramatic increase in acute rectal toxicity could be seen at 1 year follow up. Further studies will be reported later on. The issue could be whether we should move in to HYPO fractionated radiotherapy or whether we should use the conventional 2 Gy fraction and continue to dose escalate up to higher doses than 78 Gy.

Wednesday, September 28, 2005 Symposia

Gated radiotherapy

165

Clinical experience with gated breast irradiation

H. Nyström

The Finsen Center – Rigshospitalet, Copenhagen, Denmark

Adjuvant radiotherapy of breast cancer using tangential photon fields to include the breast implies a risk of late cardiac and pulmonary toxicity, in particular if the internal mammary nodes are included in the fields. By synchronising the accelerator with the breathing cycle of the patient, the treatment can be carried out in a phase of the breathing cycle that is most favourable with respect to dose reduction to non-target tissues.

The first step towards the clinical introduction of respiratory gated treatments was to investigate and compare different breathing manoeuvres, e.g. deep inspiration breath hold, end expiration free breathing and end inspiration free breathing. The importance of training and coaching of the patient was also investigated.

For end-inspiration free breathing, the heart volume irradiated to doses >50% of the prescription dose was on average reduced from 19% to 3% compared to un-gated free breathing. Similarly the ipsilateral relative lung volume was reduced from 46% to 30%. Deep inspiration breath hold did not significantly improve the dose distribution.

At Rigshospitalet gating is now a standard treatment for patients with left sided breast cancer and 59 patients have been treated so far with audio-coached, free breathing, end-inspiration gating. To monitor the breathing, the Varian Real-time Positioning Management™ System was used, both at the pre treatment planning CT-scanning and in order to gate the treatment unit. The patients were audio coached to ensure a deeper and more regular breathing.

The next step now under investigation, is to see whether visual coaching of the patients can further improve the technique and possibly facilitate margin reduction.

166

Can respiratory gating improve the quality of lung cancer treatment

G. Starkschall

Department of Radiation Physics, The University of Texas M.D. Anderson Cancer Center, Houston, USA

Respiratory-induced motion may cause lung tumors to move by as much as 2 cm. In order to ensure that the clinical target volume (CTV) is completely irradiated by the radiation treatment field, internal margins (IM) are placed around the CTV to generate a planning target volume (PTV). These margins result in the irradiation of significant amounts of uninvolved lung tissue, which has a relatively low radiation tolerance. One method of reducing the size of the IM has been to synchronize the delivery of radiation with the respiratory cycle, so that radiation is delivered only during a small fraction of the respiratory cycle.

The technique of respiratory gating requires a method for monitoring the respiratory cycle as well as a method for indicating to the linear accelerator when in the respiratory cycle the radiation beam is to be turned on and off. Respiratory monitoring can be achieved by one of several methods including the use of external fiducials, spirometry, or a strain gauge. Typically, respiratory motion is monitored for several cycles in order to estimate an amplitude and frequency of respiration. Gating levels are determined, typically at end inspiration, or more commonly, end expiration. Signals are sent to the linear accelerator from the gating system indicating that the respiratory cycle is within the gate, allowing for delivery of radiation.

Treatment planning studies have compared the amount of lung spared in gated treatments to the amount of lung spared when an internal target volume (ITV) was defined based on explicit motion of the CTV during a respiratory cycle. These studies have indicated that gating the delivery of radiation can increase the amount of lung spared provided the tumor is small ($GTV < 100 \text{ cm}^3$) and moves significantly ($\geq 1 \text{ cm}$), and that the amount of residual motion can be

essentially eliminated. Present gating techniques, in which a duty cycle of 30% - 50% is used, still result in a significant amount of residual motion as demonstrated by observation of the motion of implanted fiducials during gated delivery. Feedback-guided breath-hold (FGBH) techniques, in which the patient is trained to initiate a breath hold at a specific point in the respiratory cycle based on a display of the respiratory cycle, have the potential of significantly reducing the amount of residual motion during gating, demonstrating improvement in the amount of lung sparing as well as the potential for dose escalation.

167

In Room Measurement of 3D Motion in Lung

J.-J. Sonke, J. Wolthaus, E. Damen, J. Belderbos, J. Lebesque, M. van Herk

Department of Radiation Oncology, The Netherlands Cancer Institute - Antoni van Leeuwenhoek Hospital, Amsterdam, The Netherlands.

Purpose: Respiratory motion induces geometrical uncertainties during planning and radiation treatment of lung cancer patients. Classically, generous safety margins are used to account for these uncertainties, limiting the possibility for dose escalation. In order to increase the precision of RT, several methods have been proposed, such as targeting the mean tumor position, gating, and tumor tracking. All these methods require an accurate model of the tumor trajectory to design an appropriate treatment plan. Over the course of treatment, this model needs to be validated to address variations of the tumor trajectory. A possible approach is to implant fiducial markers in or near the tumor and measure the 3D trajectory using 2 orthogonal x-ray imaging systems. As an alternative non-invasive method, we propose the use of a cone beam CT (CBCT) scanner integrated with a linear accelerator.

Method: A CBCT scanner acquires a series of fluoroscopic images over a gantry sweep, which is then reconstructed into volumetric CT data. By sorting the breathing signal and the corresponding projections into several phase bins and reconstructing each subset of projections, a four dimensional (4D) CBCT dataset is generated, i.e., a 3D CBCT scan for each breathing phase. Next, the tumor trajectory can be measured by registering a region of interest (the delineated tumor) defined in (a phase of) the planning CT with each phase of the 4D CBCT.

We have analyzed 4D CBCT scans, consisting of 10 different breathing phases that were acquired on the linac just prior to irradiation of 4 lung cancer patients during 7-8 fractions. As a reference, a so-called mid-ventilation planning CT was used, i.e., the 3D element of a 4D CT dataset where the tumor position is closest to its mean position. The patients had an average breathing period between 2.8 and 4.5 s, and a peak-to-peak amplitude of the tumor trajectory between 1.1 and 1.6 cm.

Results: A group averaged displacement of the mean tumor position of 2.1 mm in the inferior direction was found. The systematic error (1 SD) of the mean tumor position was 1.4 (LR), 4.0 (CC) and 2.9 (AP) mm. The inter-fractional random error of the mean tumor position was 0.9 (LR), 4.8 (CC) and 3.1 (AP) mm. Inter-fractional variations of the tumor trajectory relative to the mean position were small: 1.1 mm (CC, 1 SD). As can be expected, with appropriate imaging during planning but without a correction protocol, the systematic and random errors were similar. Based on these results, an offline protocol correcting for systematic baseline shifts could reduce the safety margins from 16 to 10 mm for the patients studied.

Conclusions: We have developed a non-invasive procedure to measure the 3D tumor trajectory based on 4D CBCT. This enables the verification of this trajectory just prior to treatment. The next step is to develop methods to update the 4D patient model using a respiratory signal or fluoroscopic imaging to account for intra-fraction variability.

168

Ongoing clinical experience utilizing moderate Deep Inspiration Breath-hold (mDIBH) to reduce cardiac dose in left sided breast irradiation.

N. Letts, A. Martinez, F. Vicini, D. Yan, V. Remouchamps, J. Wong

Department of Radiation Oncology, William Beaumont Hospital, Royal Oak, MI, USA

Purpose/Objectives: Moderate Deep Inspiration Breath-hold (mDIBH), as applied using an Active Breathing Control (ABC) device, has been employed in our clinic since February 2002 to reduce the cardiac dose for patients undergoing left-sided whole breast irradiation. In this paper, we present our ongoing clinical experience, as well as data on dosimetric analysis and setup variation of the treatment technique.

Materials/Methods: Thirty-eight patients with left sided breast cancer were reviewed for treatment on our ABC treatment protocol. Of these, 3 patients were unable to complete the procedure due to severe claustrophobia, limited lung function or lack of acceptance. Another 5 did not show benefit according to the screening ABC CT scans and were not enrolled. The remaining 30 patients were treated at mDIBH, defined as 75%-80% of the maximum inspiratory capacity. All patients were treated with intensity modulated radiotherapy (IMRT), as per our standard practice. Dose volume parameters were analyzed for the heart and ipsilateral lung. The heart NTCP was also calculated. In addition, intra- and inter-fraction setup variations were quantified for all patients. Both the medial and lateral beams were split into 2-3 breath-holds for delivery, with the open beam segment deliberately distributed and delivered in 2 breath-holds. Electronic portal images (EPIs) were acquired of all open beam segments daily. The intra- and inter-fraction setup variations were derived by aligning the daily EPIs with the prescription digitally reconstructed radiographs (DRRs) using an in house treatment verification tool. Ribs and chest wall were chosen as the anatomic features for alignment.

Results: A total of 775 treatment fractions were delivered with ABC. The mean age of patients treated was 47.9 years (range 30-65). Fifteen patients received chemotherapy prior to radiation treatment. The mean number of breath-holds required per beam was 2.3 (range 2-4), with a mean duration of 17 seconds per breath-hold (range 5-25). The mean threshold level set for mDIBH was 2.0 liters (range 1.5-2.7). With mDIBH, it was possible to reduce the volume of heart receiving 30Gy (V30) by an absolute mean of 2.9% (from 3.2% in Free Breathing (FB) to 0.3% in mDIBH), and the heart NTCP by an absolute mean of 0.8% (from 0.9% to 0.1%, respectively). The mean percentage reductions of the heart V30 and NTCP values with mDIBH were 93.8% and 94.4% respectively. In 13 of the 30 patients treated at mDIBH, the heart was completely displaced from the field reducing the mean V30 and NTCP values at FB from 1.9% and 0.5% to 0%, respectively. Treatments at mDIBH and FB resulted in similar values for the volume of lung receiving 20Gy (V20) with mean values of 9.7% and 10.5% respectively. A total of 2705 EPI were analyzed. Results from the analysis of inter and intra-fraction setup variations for the 30 patients are shown in table 1. The inter-fraction variation in the cranio-caudal direction is larger than in the anterior-posterior direction, similar to the general clinical experience for whole breast treatment. As expected from our initial experience, ABC treatments do not result in an increase in inter-fraction setup variation when compared with FB treatments.

| TABLE 1 | | ANTERIOR-POSTERIOR | | | | CRANIO-CAUDAL | | | |
|----------------|--------------------|--------------------|-------|-----------|-------|---------------|-------|-----------|-------|
| | | MEDIAL | | LATERAL | | MEDIAL | | LATERAL | |
| | | BH1 | BH2 | BH1 | BH1 | BH1 | BH2 | BH1 | BH2 |
| Inter-fraction | M μ | -0.1 | -0.3 | -0.2 | -0.7 | 1.2 | 1.4 | 2.8 | 3.0 |
| | ($\sigma\mu$) | (2.3) | (2.2) | (2.3) | (2.3) | (3.4) | (3.5) | (3.4) | (3.2) |
| | M σ | 2.3 | 2.2 | 2.2 | 2.2 | 2.9 | 3.0 | 3.0 | 3.1 |
| | ($\sigma\sigma$) | (0.7) | (0.6) | (0.7) | (0.7) | (0.8) | (0.9) | (0.8) | (0.9) |
| Intra-fraction | M μ | 1.0 (0.4) | | 1.1 (0.4) | | 1.4 (0.5) | | 1.5 (0.5) | |
| | ($\sigma\mu$) | 0.8 (0.3) | | 0.8 (0.3) | | 1.1 (0.4) | | 1.2 (0.5) | |
| | M σ | 0.8 (0.3) | | 0.8 (0.3) | | 1.1 (0.4) | | 1.2 (0.5) | |
| | ($\sigma\sigma$) | 0.8 (0.3) | | 0.8 (0.3) | | 1.1 (0.4) | | 1.2 (0.5) | |

M μ : The mean of individual means

$\sigma\mu$: The SD of individual means

M σ : The mean of individual SD's

$\sigma\sigma$: The SD of individual SD's

Conclusions: With the use of mDIBH, facilitated by an ABC device, it is possible to reduce the cardiac dose in left sided breast irradiation. Daily EPI analysis indicates excellent reproducibility of the technique, with minimal intrafraction motion observed. In addition, this procedure has been widely accepted by both patients and staff, and is offered as a standard treatment in our clinic for the eligible patient.

Acknowledgements

This work was supported in part by NCI grant RO1 CA76182, Elekta Oncology Systems, the Alfred Berkowitz Fund and the Drive to Beat Breast Cancer Fund.

169

Validation of a breathing synchronized DMLC-IMRT irradiation technique by importing measured field fluences into the treatment planning system for dose reconstruction

D. Verellen, K. Tournel, N. Linthout, T. Wauters, G. Storme Academic Hospital, Vrije Universiteit Brussel (AZ-VUB) Dept. of Radiotherapy, Brussels, Belgium

Background and Purpose: Recalculating dose distributions using measured IMRT fluence fields imported into the treatment planning system (TPS) and evaluation of the technical feasibility of a prototype developed for breathing synchronized irradiation.

Material and Methods: DMLC-IMRT fluence patterns acquired on radiographic film, generated by the linac in non-gated and gated mode, have been imported into the initial TPS. The effect of possible interplay between organ motion and leaf motion and the efficacy of a breathing synchronized irradiation technique (an adapted version of a commercially available image-guidance system: NOVALIS BODY / ExacTrac4.0, BrainLAB AG) has been evaluated using radiographic film mounted to a simple phantom simulating a breathing pattern of 16 cycles per minute and covering a distance of 4 cm to obtain the resulting fluence maps. Two situations have been investigated: (a) A tumor located close to the diaphragm to assess the influence of organ motion on the dose to the target volume as well as to the gastrointestinal tract that presents a high risk at intersecting with the beam during the breathing cycle. (b) A thoracic lesion requiring complicated fluence patterns to assess the possible interplay between leaf motion and organ motion.

Results: Importing measured fluence maps yielded highly disturbed reconstructed dose distributions in case of the non-gated delivery with the phantom in motion (both orthogonal and parallel to the leaf direction), whereas the measurements from the static (film fixed in space) and the gated delivery showed good agreement with the original theoretical dose distribution. These findings have been confirmed by the dose-volume histograms, corresponding tumor control probabilities (almost identical for the original, static and gated measurements; yet reduced with a factor 2 for the "in motion and non-gated" delivery), conformity index and dose heterogeneity values (increased with a factor 3 to 6

-depending on the case- when motion was induced, whereas again similar values have been obtained applying the original, static and gated fluence maps). The normal tissue complication probability seems to be affected to a lesser degree, which concurs with the observation that the interplay effects result in a dose spread in the direction of motion. The applied breathing synchronization technique introduced an increased treatment time with a factor 3 to 4.

Conclusions: The use of measured fluence fields, delivered by the linac in non-gated and gated mode, as imported fluence maps for the treatment planning system is an interesting quality assurance tool and revealed the dramatic impact of interplay between DMLC-IMRT dose delivery and organ motion, as well as the advantage of breathing synchronization to resolve this issue. The latter should, however, be outweighed against the increased treatment time.

Basic and Novel dosimetric systems

170

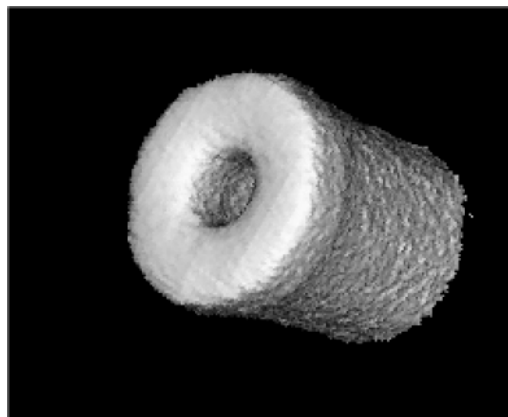
Gel dosimetry; clinical applications and basic investigations

*S.Å. Bäck, A. Karlsson, P. Haraldsson, H. Gustavsson
Department of radiation physics, Malmö University Hospital,
Lund University, Sweden*

The increasing complexity of modern irradiation treatment techniques, where high dose gradients are used in combination with small margins to a complex planning target volume (PTV), demands adequate and accurate verification of both the treatment techniques and the dose calculation algorithms. In the assessment of the dose calculation algorithms utilized in modern treatment planning systems (TPS) there is a need for three-dimensional absorbed dose measurements.

The dosimeter gels offer a great potential for the quality assurance procedure, as it measures the integrated dose distribution in three dimensions where the phantom itself forms the detector. For most applications with dosimeter gels, a gel with a density close to water is used. However, for adequate dose verification, the potential to simulate different electron densities is of great interest. This may be achieved using a low density ($\sim 0.6 \text{ g/cm}^3$) normoxic polymer gel, containing the antioxidant tetrakis (hydroxymethyl) phosphonium (THP). Results covering the basic dose response characteristics for gel compositions simulating both lung and soft tissue (water) will be presented. The response dependence with LET (linear energy transfer) will also be discussed. The potential to measure complex 3D dose distribution from a scanned proton beam were recently examined using gel dosimetry and MRI (see figure).

At present various investigators have evaluated a number of clinical applications where gel dosimetry offers unique and especially valuable features. This and possible pitfalls will be covered in the presentation. The aim of the talk is to provide a basic understanding in gel dosimetry and to show the importance of basic examination of the gel system characteristics and uncertainty estimations before going into complex treatment geometries.



171

Applications of EPR dosimetry in radiotherapy

E.S. Bergstrand

*Dept. of Medical Physics, The Radium Hospital, Montebello,
Oslo, Norway*

EPR spectroscopy may be used for detecting the concentration of radicals in materials. The EPR absorption signal reflects the concentration of radiation-induced free radicals, a concentration which is an approximately linear function of the absorbed dose in the material for a wide dose range. When the amino acid alanine was introduced as an EPR dosimetry material, EPR/alanine was considered to be a potentially important solid state dosimetry system for radiotherapy applications. This view relates to the advantageous dosimetric properties of EPR/alanine; the wide linear dose range, the rather water equivalent energy absorption properties, the low fading rate and small dependence of e.g. dose rate, and the possibilities concerning readout without removing the signal. In general, EPR dosimetry has shown to have a wide range of applications, covering geological dating, retrospective dosimetry, and high-dose dosimetry. However, any large-scale replacement of existing dosimetry systems by the EPR/alanine system has not taken place for radiotherapy applications. One cause of explanation is probably the low sensitivity for EPR with alanine in the subgray range, which limits its use for routine in vivo dose measurements of patients receiving fractionated radiotherapy. Although precise measurements in the subgray range have been demonstrated with alanine, the precision is commonly gained on account of the exceeding time thus required for signal evaluations. However, when providing quality assurance in radiotherapy, there are numerous examples besides routine in vivo dosimetry where a physicist will be in need of a tissue equivalent dosimeter. E.g., when verifying the dosimetry of new treatment techniques, or when checking the validity of a dose calculation, EPR dosimetry offers precise and accurate measurements of up-scaled doses in phantoms. EPR dosimetry is also suited for performing dose comparisons among different centers, e.g. when comparing outcome of different treatment regimes.

The talk will give a short introduction to the method of EPR dosimetry and show some of the variety of applications. Some of the experience with alanine as an EPR dosimeter will be discussed, and examples given of new candidates for more sensitive EPR dosimetry materials.

172

Novel Dosimetry Measurement Systems

G.S. Ibbott

*U.T. M.D. Anderson Cancer Center, Department of Radiation
Physics, Houston, USA*

With the current trend toward treatment with small, complex, and dynamic radiation fields, the need to make 2D and 3D measurements, as well as point measurements in or near steep dose gradients, has grown significantly. Intensity-modulated radiation therapy (IMRT) in particular requires that 3D measurements be performed to confirm that the

complex algorithms and delivery techniques are accurate. Because of complex modulation of dose across the treatment fields, measurements make demands that exceed the capabilities of many conventional technologies. Stereotactic radiosurgery (SRS) fields, which are smaller than many conventional detectors used in radiotherapy, require special measurement techniques. Novel dosimeters, including micro ionization chambers, diamond detectors, MOSFETs, gel dosimeters, high precision film systems, electronic imagers and detector arrays will be discussed as they relate to the special measurements necessary for IMRT, SRS and 3D conformal therapy. The accuracy of these measurement devices and techniques will be important to the practicing radiotherapy physicist as new treatment and calculation techniques are introduced in the clinic.

173

Delivered Dose Reconstruction with MV cone-beam CT

J. Pouliot

Department of Radiation Oncology, Univ. of California, San Francisco, USA

Elaborate methods of patient imaging, dose calculation, and radiation delivery are currently used to develop treatment plans with highly conformal patient dose distributions. However, the true delivered dose likely deviates from the planned distribution due to differences in patient position, anatomic changes due to weight loss or tumor shrinkage or variations of linac output during treatment. In the presentation, we will discuss our method to reconstruct the delivered dose from measurements made during treatment, leading to the development of Dose Guided Radiation Therapy (DGRT), an adaptive strategy where dosimetric considerations constitute the basis of treatment modification. The proposed dose reconstruction method uses a Megavoltage cone-beam computed tomography (MV CBCT) image acquired on the treatment table prior to treatment, 2D portal images taken with an amorphous-silicon electronic portal imaging device (EPID) during treatment, and an independent validated dose calculation engine. The MV CBCT image should provide a more accurate depiction of the patient in the true treatment-time position as well as the necessary photon attenuation coefficients for dose calculations. The treatment-time portal images provide information on the true (photon) fluence pattern delivered by the linear accelerator.

For the acquisition of MV CBCT images, the firmware and operating parameters of a linac are adjusted to allow delivery of fractions of a Monitor Unit per segment. The flat panel detector acquires images synchronized with the linac beam. A series of 2D projection images, one image per degree for 200 degrees, are acquired. The total exposure from this procedure can be made as low as 2 cGy. The 3D volume is reconstructed using a cone-beam reconstruction algorithm.

To infer the delivered energy fluence, the flat panel is used to collect portal images during treatment. The images are corrected for inhomogeneous pixel sensitivity, detector scatter, and the panel's energy response. The signal is converted to energy fluence by calibrating the detector using ion chamber measurements. The energy fluence is then back-projected through the attenuation coefficient calibrated CBCT volume. The energy fluence is corrected for the $1/r^2$ falloff as well as for patient attenuation using the MV CBCT data. Finally, a superposition/convolution energy deposition method is used to calculate the dose.

Dose reconstruction combined with low-exposure MV CBCT has great potential to provide verification and possible improvement of dose delivery in patients with virtually no additional hardware. Knowing the true delivered dose distribution will enhance our understanding of treatment outcomes. Moreover, adaptive methods such as DGRT will be developed to adjust treatment plans midcourse to compensate for differences in delivered and planned doses, improving treatment accuracy. Details of the procedure and first clinical results of dose reconstructed will be presented.

IMRT of the pelvis

174

Intensity Modulated Radiotherapy for gynaecological malignancies

D. Georg, P. Georg, M. Hillbrand, K. Dieckmann, R. Pötter
Dept. Radiotherapy and Radiobiology, Med. Univ. Vienna, Austria

Purpose: To evaluate the impact of IMRT and different delineation strategies for intestine in patients with gynaecological malignancies. Additionally, variations in dose constraints for inverse planning were assessed.

Methods and Materials: Five women with cervical cancer treated with definitive radiotherapy ('def') without concomitant chemotherapy and five women with endometrial cancer treated postoperatively were selected ('post'). For each patient a planning CT was made with oral and intravenous contrast and a full bladder. The CTV was defined according to the department's protocol and the PTV was defined as CTV plus a 1 cm safety margins in all directions. Bladder, rectal wall and sigma were contoured as single structures. Small bowel and colon, except of sigma, were delineated as single loops. Additionally, because these structures are mobile we delineated the 'intestine' as a peritoneal cavity. A conformal four field plan (4F) and an IMRT plan (7 beams) were made for each patient using CMS XiO. Both plans were normalized to deliver 50.4Gy in 1.8Gy per fraction to the PTV.

Results: The delineated volumes of intestine, small bowel and colon did not differ between both groups. At the prescription dose level, the average irradiated volume of intestine was reduced by the factor of 8 when comparing IMRT and 4F: 3.5% vs 27.7% def, 2.5% vs 20.7% post. A similar reduction was observed for small bowel and colon, delineated as single loops. For the sigma and the rectal wall doses >50.4Gy could be reduced by the factor of 2. Bladder sparing at the prescription dose level differed in postoperative and definitive RT patients (28% vs 61.4% def; 19.4% vs 75.8% post). In the patient group with definitive RT mean doses to the intestine were 34.7Gy using IMRT and 36.6Gy for the 4F plan. Corresponding values in the postoperative group were around 32Gy for both IMRT and 4F. The average mean doses for sigma, rectal wall and bladder were around 47Gy for IMRT and about 50Gy for 4F plans, for patients receiving definitive RT. For gynaecologic IMRT applications anatomy variations, i.e. organ size, PTV size and shape, etc. influenced the variation of dose and DVH constraints for inverse planning. Artificial 'help' structures were found to be useful to improve dose conformity or OAR sparing.

Conclusion: Our results suggest that the delineation of 'intestine' is sufficient and time sparing for IMRT planning of patients with gynecological malignancies. Conformal sparing in the high dose region of intestine, sigma, rectal wall and bladder could be significantly improved using IMRT. Dose constraint templates can be established for inverse planning of gynaecological malignancies and used as a 'good starting point' to run optimization.

175

Pelvic IMRT for Gynaecological Cancer – An Oncologist's View – A Uro-Oncologist's View

J. Staffurth

Clinical Senior Lecturer in Oncology, Cardiff University, UK

Background

Whole pelvic radiotherapy (WPRT) is routinely used in the management of patients with gynaecological malignancies in three clinical scenarios: locally advanced cervical cancer, cervical cancer patients requiring post-operative WPRT and endometrial cancer patients requiring post-operative WPRT. In order to maximise the dosimetric advantages that intensity-modulated WPRT (IMWPRT) offer, the precise clinical issues must be fully understood.

Other advances: Screening and vaccine programmes may reduce the absolute numbers and presenting stage of patients diagnosed with cervical cancer. Advanced imaging

modalities (MRI, PET, SPECT etc) and new contrast agents (e.g. USPIO for MRI) should improve staging. Concurrent chemo-radiation has a proven role for advanced cervical cancer and its role in the adjuvant setting in high-risk endometrial cancer is the subject of an ongoing EORTC trial.

Dosimetric advantages of IMWPRT: IMWPRT reduces the volume of small bowel, bladder and rectum irradiated compared to conformal WPRT. The bone marrow containing areas of the pelvic bones can be specifically avoided without compromising normal tissue avoidance or target coverage. IMWPRT can be used to deliver concomitant boosts to the primary and sidewall or nodal disease.

Clinical challenges of IMWPRT

Target volume definition: IMWPRT requires a new concept of target volume definition as use of the standard 4-field pelvic brick becomes outdated. New imaging modalities should be evaluated and, if useful, integrated into the process. Detailed knowledge of physiological internal organ motion of targets and normal tissues is required to ensure that appropriate margins are used. Approved protocols should be developed.

Optimal use of dosimetric options: What is the best way to escalate dose? Local tumour, nodal or volume escalation, or perhaps hypofractionation or the introduction of concurrent chemotherapy? Of course not all patients require dose escalation: we should also aim to reduce the risk of toxicity for those with a good prognosis.

Widespread uptake: IMRT is complex to introduce and initially is resource intensive. Training is essential and quality assurance time-consuming. How will departments fund IMRT and which patients should be prioritised? Although the dosimetric benefits are unquestionable, what is the best way to improve patient outcome? How should IMWPRT be evaluated? How can the medical community convince the funders of European Healthcare that IMWPRT is a worthwhile investment?

176

IGRT for rectal carcinoma

*S. Roels, T. Depuydt, S. Stroobants, K. Haustermans
Department of Radiation Oncology, University Hospital
Gasthuisberg, Leuven, Belgium*

Neo-adjuvant chemoradiation therapy combined with TME surgery has proven to further decrease the local recurrence rate, compared to TME alone [2,3]. However in high-risk patients, local recurrence ranges from 0-33% [4] with trimodality treatment, demonstrating room for improvement in therapy.

As radiotherapy is part of the preoperative strategy, radiation treatment optimisation can contribute to improvement in local control. Four different issues of this treatment optimisation process will be discussed.

I. Development of bio-image guided optimisation of radiation therapy for rectal cancer

As most loco-regional relapses in high-risk patients still occur in high dose regions [5,6], it is interesting to develop methods to detect the radiation resistant regions of the tumour and to target these regions using a higher biologically effective dose. We aim to develop intensity modulated radiation therapy (IMRT) optimisation by dose painting to areas at high risk based on PET signal intensity with different PET tracers (that provide information on radiation resistance). Sequential PET-CTs with F-FDG, F-MISO and FLT are performed during the preoperative therapy. These images allow us to determine biological important tumour areas and compare anatomical and functional tumour definition and delineation. Next to that, we look how these 'hot spots' evolve during radiotherapy by assessing changes in PET signal intensity throughout the treatment course.

II. Development of Intensity Modulated Radiotherapy (IMRT) for rectal cancer

We will develop IMRT planning for the treatment of rectal cancer using different equi-spaced static beams using the commercial planning system Eclipse (Varian). These beams will be configured around the PTV and the biological PTV, as defined on PET scan (see I), delivering a higher dose per fraction to the biologically active tumour volumes (SMART-technique). A planning study will demonstrate and evaluate the dose distribution compared with conformal 3D techniques

with respect to the target volumes and critical structures.

This planning process approach is totally different from the Intensity Modulated Arc Therapy (IMAT) technique. The comparison of both approaches regarding planning time, dose distribution and dose delivery will allow us to define the best option to fully exploit the bio-image guided treatment process.

III. Set-up variation and rectum shape variation

Introduction of IMRT into treatment planning will introduce steeper dose gradients across the volumes of interest and demand a very accurate and reproducible patient positioning. Patients irradiated for rectal cancer are currently treated at our centre in prone position by use of a belly board device in order to spare the maximum amount of small bowel volume in high dose areas. The results of different set-up verification and correction protocols at our center are within the limits described in literature for pelvic treatments and will be presented.

However, even the most accurate patient positioning cannot prevent internal organ variation throughout a course of radiotherapy. This can cause a significant difference in the actual dose delivered from the precalculated dose. The influence of shape variations of the rectum on the actual delivered dose depends on the dose gradient around the rectum. When the gradient across the rectum becomes steeper, using IMRT, it becomes important to ensure adequate daily target covering. A study on variation of the rectum shape using on board imaging (OBI) throughout a course of radiotherapy will provide us information to define margins for the PTV.

177

IMRT for prostate cancer

A. Heaton

*Radiotherapy Department, Clatterbridge Centre for Oncology
NHS Trust, Merseyside, UK*

Introduction: IMRT is becoming the treatment option of choice for prostate cancer due to a commonly concave target volume and the proximity of organs at risk. Over 100 patients have received this treatment to date at Clatterbridge Centre for Oncology (CCO). This presentation details the experience gained implementing IMRT and expected developments in the area.

Planning: Patient selection and outlining protocols will be discussed along with planning techniques used at CCO. The use of inverse rather than forward planning techniques require new skills in the identification of dose constraints for targets and organs at risk and a familiarity with the representations of dose distributions by dose volume histograms. A CCO class solution has been developed and will be presented.

Organ motion: Patient and organ motion and the accuracy of target positioning have direct implications for the probability of local control and for the dose received by organs at risk. An overview of the types of organ motion to consider will be discussed relevant to prostate IMRT: position-related, interfraction and intrafraction. Methods that can be used to solve them will be suggested and will include the effect of bladder and rectal filling, the use of radio-opaque markers and cone-beam CT.

Quality Control (QC) and Verification: Initial commissioning and routine QC will be considered and the practical aspects of delivering this treatment modality including on-treatment imaging.

Departmental Implications: In the UK, obstacles identified as preventing implementation of IMRT into the department include equipment availability, staff shortages and the increased time required for each step in the process. With greater familiarity and experience QC time, in particular is likely to be reduced as more efficient methods are developed. The development of class solutions will also result in a reduced amount of time being required for treatment planning.

Future Developments: Future developments are discussed which include the role of radiobiological optimisation and image-guided radiotherapy techniques.

178

IMRT-planning of anal carcinoma*E. Lamers-Kuiper, B. Mijnheer, L. Dewit**Department of Radiation Oncology, The Netherlands Cancer Institute, Antoni van Leeuwenhoek Hospital Amsterdam, The Netherlands*

Purpose: To improve dose homogeneity within the planning target volume (PTV) and to achieve normal tissue sparing in radiation treatment of anal carcinoma using IMRT.

Method: Two case reports are presented in whom the radiation dose distribution in the pelvis is compared between a standard and an IMRT technique.

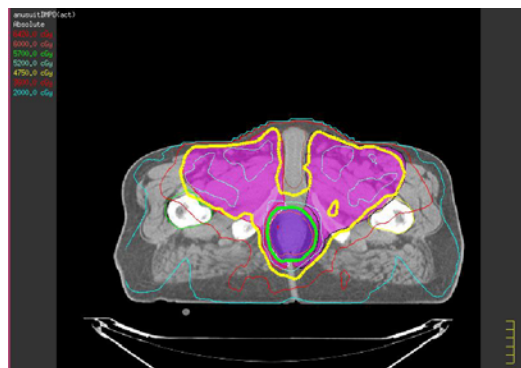
Axial CT-slices are used for delineating the PTV. A standard 5-field technique is used, with one posterior and two lateral 18 MV photon fields for the posterior pelvis and two anterior electron fields for the inguinal lymph node area.

A 7-field IMRT technique is applied including a simultaneous integrated boost. The prescribed total dose to the regional lymph nodes is 49.5 Gy in 33 fractions of 1.5 Gy, whereas the dose to the primary tumor is 59.4 Gy in 33 fractions of 1.8 Gy.

Results:

Using the standard technique, an unacceptable large underdosage (up to 50%) is observed in the region between the pelvis and the inguinal lymph node area. In addition, unnecessarily high doses are given to surrounding normal tissues, most notably to the genital area. In contrast, with the IMRT technique a homogeneous dose distribution is obtained in the PTV (D95=98.9% for the inguinal lymph node area and 98.0% for the tumour area with a maximum dose of 104.5%) with significant sparing of the genital area (46% of the prescribed dose).

Conclusion: IMRT with an integrated simultaneous boost for anal carcinoma is the radiation treatment technique of choice, in particular when the inguinal lymph nodes are included in the PTV.



Gating in radiotherapy

179

Quality Assurance of 4D-CT using a programmable motorized phantom

L. Simon¹, P. Giraud², A. Mazal¹, J. Rosenwald¹

¹Institut Curie, Service de Physique Médicale, Paris, France

²Institut Curie, Service de Radiothérapie, Paris, France

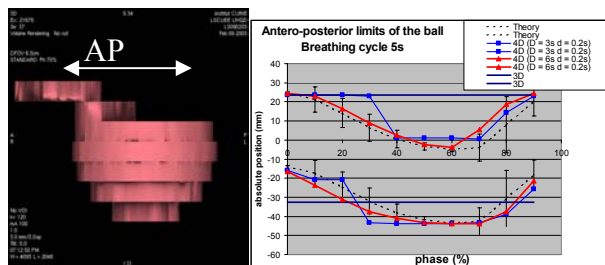
Four-dimensional Computed Tomography (4D-CT) is a new acquisition mode used in radiotherapy of intra-thoracic organs to study motion induced by patient breathing. It allows to reconstruct 10 full series at different phases of the breathing cycle. On the patient's chest, an external marker (RPM system, Varian), used as a surrogate of the motion, is followed by an infra-red camera. The RPM signal is used to sort CT images acquired in cine mode. Each slice is acquired during a *cine duration* (D), usually recommended to be chosen as the time for full breathing cycle plus tube rotation (TR). With the same values of D and TR , it is possible to reconstruct a variable number N of images per slice, by changing the *cine interval*, (CI) (see equation). CI is the time delay between two consecutive reconstructed images.

$$N = \frac{(D - TR)}{CI} + 1$$

The phantom mimics a lung tumour. It consists of a ping-pong ball, filled with resin (1.02 g/cm^3), placed in the centre of a cubic cork block (0.24 g/cm^3). The block was attached to an insert actuated along a linear slider by a programmable motor. An analytic breathing motion was implemented (see dashed lines on figure). Only antero-posterior (AP) motions were investigated. Acquisitions were made with 1 second tube rotation time, using both 3D-CT and 10 phases 4D-CT. Different D , CI and slice width values were used for each phantom motion sequence. Ball volumes and absolute positions of the AP limits were compared to the expected values obtained from phantom geometry and from programmed positions.

In presence of motion, the ball volume was systematically over-estimated by CT: 8% for 3D-CT, and from 1% (at end expiration) to 29% (at mid inspiration) for 4D-CT. However, even when the total volume was correct, if D was too small (i.e. $<$ breathing cycle), the object position could be incorrectly represented on some slices (see image), and could result in an overestimation of the AP diameter of the moving ball greater than 1 cm (see figure). For larger values of D the absolute positions of the AP limits of the ball was consistent with the programmed positions. Diameter overestimation was 41% on 3D-CT and only 0-2% on 4D-CT at extreme phases if parameters were properly chosen.

A programmable and multi-usage phantom was developed which could follow simple analytical and complex motions (e.g. extracted from 11 consecutive breathing cycles of a real patient). This phantom helps to choose the CT acquisition parameters, to evaluate the performances of 4D-CT reconstruction and the overall quality of the treatment chain.



180

Accuracy of predicting respiratory tumor motion with the Synchrony/CyberKnife tumor tracking system

Y. Seppenwoolde, D. Jansen, H. Marijnissen

Erasmus MC - Daniel den Hoed Cancer Center, Rotterdam, The Netherlands

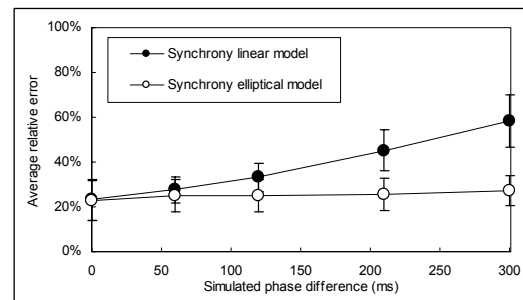
Background: Synchrony is the system of the CyberKnife robotic treatment device to irradiate extra-cranial tumors with respiratory motion. The advantage of Synchrony is that patients can breathe normally throughout treatment while the CyberKnife robot actively compensates for breathing motion (tumor tracking).

Methods: The system continuously tracks the position of external infrared LED markers. Before treatment, 3 to 10 X-ray images of implanted gold seeds are acquired to obtain a linear correlation function between in- and external motion. During treatment, X-ray images are acquired regularly to update the model. If the correlation between in- and external motion is perfect, it is sufficient to track only the external motion to accurately predict the internal tumor position. However, if there exists a phase difference between in- and external motion, or if the tumor moves with hysteresis, a linear model may not be accurate enough.

In a simulation study, using 3D breathing patterns of 8 patients (treated with real-time-tumor tracking radiotherapy) with tumor motion larger than 5 mm, the influence of phase differences on the prediction error of the synchrony system was investigated. A new model was proposed, which uses an elliptical function instead of linear correlation. An artificial LED signal was constructed by adding the amplitudes of the tumor motion in all 3 directions quadratically. This signal could be shifted in time, mimicking a phase-difference between in- and external motion.

Results: With the Synchrony system, the average 3D error between predicted and actual tumor position during treatment can be reduced to $\pm 25\%$ of the error made without any breathing compensation. The residual error was due to noise and breathing irregularities. Phase differences between in- and external signal of less than 120 ms have only limited influence on the treatment error. For the linear prediction model, phase differences of 300 ms increase the treatment error to $\pm 60\%$. With the elliptical model, the treatment error stays low, even for phase differences larger than 120 ms. For patients with internal hysteresis, the elliptical model performed slightly better than the linear model.

Conclusions: In theory, the Synchrony system accurately tracks tumor motion, even if a limited phase difference between in- and external motion is present. An elliptical prediction model can further reduce treatment errors due to breathing in case of larger phase differences or hysteresis.



181

Adaptive neuro fuzzy inference system (ANFIS) for prediction of respiratory motion

M. Kakar¹, H. Nyström⁴, L.R. Aarup⁴, T.J. Nøttrup⁴, D.R. Olsen^{1,2,3}

¹Department of Radiation Biology, Norwegian Radium Hospital, Montebello, Oslo, Norway

²Department of Medical Physics and Technology, Norwegian Radium Hospital, Oslo, Norway

³Department of Physics, University of Oslo, Norway

⁴Department of Radiation Oncology, The Finsen Centre, Rigshospitalet, Copenhagen, Denmark

The quality of radiation therapy delivered for treating cancer patients is related to setup errors and organ motion. Due to the margins needed to ensure adequate target coverage,

many breast cancer patients have been shown to develop late side effects such as pneumonitis and cardiac damage. Breathing adapted radiation therapy offers the potential for precise radiation dose delivery to a moving target thus reducing the side effects substantially. However, the basic requirement for breathing adapted radiation therapy is to track and predict the target as precisely as possible. Recent studies have addressed the problem of organ motion prediction by using different methods including artificial neural network and model based approaches. In this study, we propose to use a hybrid intelligent system called ANFIS (Adaptive Neuro Fuzzy Inference System) for predicting respiratory motion in breast cancer patients. In ANFIS, we combine both the learning capabilities of neural network and reasoning capabilities of fuzzy logic in order to give enhanced prediction capabilities, as compared to using a single methodology alone. After training and validating with ANFIS, the average RMSE (Root Mean Square Error) was found to be 35% of the respiratory amplitude for the un-coached patients and 6% of the respiratory amplitude for the coached patients. It was also found that the prediction accuracy, averaged over 11 breast cancer patients, was reduced to sub-millimeter over a period of 20s provided the patient was assisted with coaching.

182

An "in silico" clinical trial comparing free breathing, slow and respiratory correlated computed tomography in lung cancer patients

G. Bosmans, J. Buijsen, A. Dekker, M. Velders, L. Boersma, D. De Ruysscher, A. Minken, P. Lambin
 Dept of Radiation Oncology (MAASTRO Clinic), GROW, University Hospital Maastricht, Maastricht, The Netherlands

Purpose: The use of respiration correlated CT (RCCT) makes it possible to quantify tumor motion, allowing margin individualization. In this study we compared 4 different datasets of target delineation. The aim is to determine which method resulted in the highest mean tumor dose and good tumor coverage, respecting normal tissue constraints for lung and spinal cord.

Patients & Methods: In 9 patients treated for NSCLC, both a free breathing (FB) CT scan and an RCCT were acquired on a modified Siemens Sensation 10. For each patient treatment plans are made based on different methods of internal target volume (ITV) delineation: a conventional FB-CT (with standard margins for tumor motion), a slow-CT (no margins for tumor motion), the complete 10-phase (10ph) CT (no margins for tumor motion) and the half-ventilation (HV) CT (with an individual internal margin of (motion amplitude/4)). These plans were projected on all the respiration phases to estimate the actually delivered tumor dose and tumor coverage. Furthermore, set-up margins are added to create different PTV's and the Mean Lung Dose (MLD) was determined for each plan, for a prescribed tumor dose of 70 Gy. Subsequently, tumor doses were escalated for a fixed MLD of 15 Gy.

Results: Detailed analysis of minimum doses and cold spots learned that a significant under dosage (<95%) occurred using the slow-CT based treatment plan in one patient with the largest tumor motion (15 mm amplitude). Using the FB-CT scan, the MLD was significantly higher for all patients than using the slow-CT, HV-CT or 10ph-CT (14.4±1.5Gy vs 12.7±1.5Gy, 13.2±1.7Gy and 13.7±1.5Gy, p=0.008; p=0.012; p=0.021, respectively). Dose-escalation resulted in a tumor dose of only 73.5 Gy for the FB-CT, while higher doses could be reached using the other plans (84.0 Gy, 80.7 Gy and 77.6 Gy for the slow-CT, HV-CT en 10ph-CT respectively).

Conclusion: Use of the half-ventilation CT, with individualized anisotropic margins based on tumor motion, makes it possible to escalate tumor dose. Since treatment planning based on slow-CT may lead to under dosage in some tumors and the delineation of the 10ph-CT is rather cumbersome, we conclude that using the HV-CT is the most suitable method for radiation treatment planning in lung cancer patients.

183

Clinical feasibility of a proposed internal margin model to account for variability in respiratory motion in gated radiotherapy delivery

C. Coolens¹, P. Evans², S. Webb², M. Bidmead¹
¹Royal Marsden Hospital Trust, Physics, London, UK
²The Institute of Cancer Research and Royal Marsden Hospital Trust, Physics, Sutton, UK

Purpose: To design an internal margin model to account for variability in respiratory motion in gated radiotherapy delivery and to assess the clinical feasibility of the derived patient-specific margins.

Method and Materials: A statistical model was developed to account for the variability in breathing amplitude and phase and hence design the minimum motion margin needed for treatment. By using a polar coordinate system a gating window parameter could be included. The model uses real-time tumor position variations, which can be observed under fluoroscopy or with 4D CT scanning. The model was tested initially with a tumor motion pattern derived from the abdominal movement of a liver patient (measured over 3 min with the Varian RPM system) and is currently under investigation with fluoroscopy and CT data for various breast and liver patients.

Results: Analysis of the margins derived with the RPM data show that the margins needed for variations in phase are in the order of a few millimeters but could increase significantly when large gating windows are used (e.g. 8.6 mm for a 50% window around exhale). With time a drift was visible in the duration of the breathing cycle which could lead to a larger variation in phase reproducibility. The model-based margins did reveal a significant reduction in size compared to the standard Cartesian margins.

Conclusion: The developed model allows to create a patient-specific motion margin for the variability in breathing motion during gated radiotherapy treatment. By using the gating coordinate system, margins could be kept to a minimum, resulting in an approximately 10-fold decrease compared to standard margins in Cartesian planning coordinates. This will benefit the sparing of normal tissues but also allow for optimization of the most efficient gating window size. In addition, the model is able to detect changes in the breathing level, i.e. the average tumor position with time. With the advent of cone-beam CT capabilities in the treatment room, one could envisaged the predictive power of this model when it comes to quickly assessing the validity of the margins as calculated pre treatment and the possibility of adopting treatment if needed.

184

An analysing software for determining the parameters for respiration-gated radiotherapy

A. Block, R. Bauer
 Klinikum Dortmund, Division of Medical Radiation Physics, Dortmund, Germany

The intrafraction organ motion and its management presents a challenge for radiotherapy. The largest organ and target motion are observed in thorax and abdomen region. If such organ movement is not properly accounted for during the radiation treatment planning process, underdosed target volume will reduce the probability of cure and overdosed healthy tissue could increase the danger of radiation complications. In order to achieve a homogeneous dose to the CTV throughout the course of irradiation, CTV-PTV margins must be added.

Our approach to improve the treatment accuracy for targets in lung and abdomen is to gate the accelerator to the respiratory motion with a marker block as a surrogate indicator. A necessary requirement is to combine the external respiratory waveform with the internal tumour motion. For this job we developed the software tool ORAT, based on Microsoft VisualBasic Version 6. This software enables us to quantify the respiration amplitude in all space directions and therefore allows calculation of patient-individualized margins compensating respiratory induced displacements.

Our in-house developed software ORAT has to synchronize

and analyse images of the simulator sequenced live fluoroscopy and respiration data of the external marker block. For the display of the images and video sequences the Microsoft MediaPlayer V6.4.09.1125 is used. The data analyses yield us information about the extend of motion of the target in the cranio-caudal direction. The clinician has to mark a defined anatomic structure within the GTV in each of the simulator images. The software ORAT allows describing a possible phase shift between the respiratory and tumour motion pattern and therefore enables the decision, whether to use phase or amplitude tracking of the respiratory signal. To determine the amplitudes and frequencies of medio-lateral and ventro-dorsal target movements, we perform after the planning CT a free breathing single slice CT sequence of one minute. After marking well defined anatomical structures by a clinician, the above mentioned in-house developed software tool will analyse and evaluate this sequence. For the individualized assessment of the CTV-PTV margin we follow McKenzie et al. (The British Institute of Radiology) who proposed the idea, that the breathing positional error should be combined linearly with the other errors. In the last step for monitoring the gated treatment, our software analyses a portal imaging sequence after treatment.

185

A concept for the estimation of dose uncertainties caused by respiratory motion in radiotherapy

J. Unkelbach, U. Oelfke

German Cancer Research Center (DKFZ), Medical Physics in Radiation Oncology, Heidelberg, Germany

Introduction: In the presence of organ movements during radiotherapy, the dose delivered to a volume element of tissue becomes a stochastic property which can to a first approximation be assessed by means of an expectation value and a variance. The expectation value is typically calculated by convolution methods. We present a theory to additionally estimate dose uncertainties, i.e. the dose variance in radiotherapy due to respiratory motion.

Materials and Methods: The method applies the motion model proposed by Lujan et al (1999). The position r of a volume element as a function of time t is described by

$$r = r_0 + A \cos^{2n} \left(\pi \frac{(t + \phi)}{T} \right) \text{ where } T \text{ is the period. For a}$$

finite time of irradiation starting at $t = 0$, the delivered dose depends on the starting phase ϕ . Furthermore, the exhale position r_0 and the amplitude A will be subject to fluctuations. Hence, the expected dose $\langle D \rangle$ will not be realized after the irradiation but is associated with a variance. We assume that A and r_0 scatter around a mean value according to a normal distribution whereas ϕ is uniformly distributed.

Results: We derive approximate expressions for the variance $\langle D^2 \rangle - \langle D \rangle^2$ of the dose that arises from the

uncertainty in the model parameters A , r_0 and ϕ . For an idealized geometry we demonstrate the spatial and temporal dependence of the different contributions to the total variance and discuss the relative importance of the sources of uncertainty.

As a potential application of the method we consider the incorporation of organ motion into inverse planning by means of a probabilistic treatment plan optimization. Regarding this approach, the term $\left(\langle D \rangle - D_{pres} \right)^2 + \langle D^2 \rangle - \langle D \rangle^2$ is

minimized for each tumor voxel. Hence, the variance of the dose serves as a regularization term that controls the robustness of the treatment plan, i.e. it ensures that the expected dose $\langle D \rangle$ which shall be close to the prescribed

dose D_{press} is actually delivered to the voxel.

Conclusions and Outlook: The method may be used to

estimate dose uncertainties due to respiratory motion in conformal radiotherapy and step&shoot IMRT. This may be interesting especially when IMRT sequences consist of many small segments that are irradiated for a short time. The method may further be applied in IMRT treatment planning when the respiratory motion is incorporated into the optimization.

186

4D models of respiratory motion for use in RT planning and their advantages over 4DCT techniques

J. McClelland¹, J. Blackall¹, S. Hughes², S. Ahmad², D. Landau², D. Hawkes¹

¹University College London, Centre for Medical Image Computing, London, UK

²Guy's & St Thomas' Hospitals NHS Trust, Department of Radiotherapy, London, UK

Respiratory motion is a major factor contributing to errors and uncertainties when planning and delivering radiotherapy (RT) treatment for lung cancer. This abstract presents a novel method of building patient specific motion models based on non-rigid transformations. These model the motion and deformation that occurs over the Respiratory Cycle (RC), and help facilitate more accurate RT planning.

There is considerable interest in methods of acquiring 4DCT volumes for use in RT planning. The motion models presented here have many potential advantages over 4DCT methods presented to date. 4DCT methods attempt to form several complete volumes each at a pre-defined point over the RC whereas the motion models deform a single reference volume to predict the volume at any desired point over the RC. This means that the motion models are continuous over the RC, target delineation on the reference volume can be propagated over the RC, dose maps calculated at any point in the RC can be mapped back to the reference volume and they need a lot less memory than 4DCT. Measurements of target displacement and inter-cycle variability may be directly obtained from the motion models.

In our method, free-breathing (FB) CT scans are acquired in cine mode, using 3-4 couch positions to obtain 'slabs' of 16 1.5mm slices covering the region of interest (ROI). For each slab, 20-30 FB volumes are acquired over ~20s. A respiration signal is simultaneously acquired using an IR tracking system with a passive marker attached to the patient's chest, and this is used to assign each FB volume a position in the RC. Additionally a high quality reference volume is acquired at breath hold covering the whole lung, and is non-rigidly registered to each of the FB volumes using a registration algorithm based on free form deformations using B-splines. The motion model is then constructed by fitting a periodic function, based on approximating B-splines, to each of the registration parameters over the RC. Fitting the function averages out some of the inter-cycle variation, and enables the value of the registration parameters, and hence the non-rigid transformation to be calculated at any desired position in the RC. The transformation for each slab can then be calculated and applied to the reference volume to obtain a prediction of the entire ROI.

Motion models have been built for six patients. At the time of writing, detailed analysis has been carried out on one patient. The registration results were judged to have a maximum error of 3mm. The errors between the motion model and registration results caused by inter-cycle variations were within 1.7mm.

187

IMRT Treatment with Respiratory Gating. Renal lesion: a case study

T. Djemil, A. Mahadevan, L. Ponsky
Cleveland Clinic, Cleveland, USA

Objective: Clinical implementation of radiotherapy treatment of cancers using respiratory-gated IMRT. Description of a renal lesion case.

Method and materials: A 51-year-old female presented with a small left renal lesion. A 1 cm Visicoil gold marker was implanted into the tumor as a fiducial using CT. The tumor

received 16 Gy in 4 fractions BID using Novalis IMRT as part of a radiosurgical ablation protocol (dose escalation study.) The four fractions were delivered in respiratory gating mode. Target excursion with breathing was evaluated under fluoro and estimated to be about 2 cm in the sup/inf direction and 5mm in the radial direction. The patient was scanned with 7 reflective infrared markers carefully placed on the thorax/abdomen area. The PTV was obtained by adding a 10 mm margin in the superior/inferior direction and 7.5 mm in the radial direction of the CTV. An IMRT plan with a five coplanar beam arrangement was generated. The plan was delivered on a phantom in gated mode for verification using both ion chamber measurements and film. The breathing was simulated using a dynamic phantom. During treatment, the gating window was set at exhalation with an approximate tumor motion of +/- 7 mm from the gating reference level. A verification portal was taken for each beam using an Enhanced Contrast (EC) film combined with an EC verification portal fast cassette.

Results: A complete study of treatment using respiratory-gated IMRT of a renal lesion was described. Breathing studies were done to quantify target motion. The visicoil was easily identified on the portal film. The duty cycle was set to 50 % of the respiratory amplitude. Imaging, planning, verification, and treatment delivery were described. The PTV volume was reduced by 42%. The homogeneity index was 1.15. The inhomogeneity index was 1.18. The treatment time was about 25 minutes.

Conclusion: Combining IMRT with respiratory gating is highly desirable in some clinical situations. This method reduces significantly safety margins and consequently toxicity. The step-by-step implementation of the technique was described in the case of a renal lesion. This approach is feasible for clinical use and studies are underway to apply the same method to other sites (lung and liver.)

Dose computation II

188

Energy and intensity modulated electron radiation therapy by means of a Monte Carlo routine

A. Leal Plaza¹, C. Ma², F. du Plessis², J. Lagares¹, J. Li²

¹Universidad de Sevilla / Hospital Virgen Macarena, Dept. Fisiología Médica y Biofísica, Sevilla, Spain

²Fox Chase Cancer Center, Radiation Oncology, Philadelphia, USA

Introduction: Classical disease sites treated with electrons like Breast Cancer do not result in a special benefit of IMRT. Photon tangent fields frequently used to avoid lung and heart, demand a high breathing margin, which could be reduced using more perpendicular beams. The dose fall-off in the electron depth dose curve could be used to treat breast cancer using different beam energies together intensity modulation (MERT). Bolus manually changed with multiple fields do not possible an automatic procedure, so the intensity modulation has to be done with a MLC. The leaf scatter effect is essential for an electron modulated optimization method, so the developing software will be dependent on the considered MLC. One of the advantages of using a photon MLC would be the possibility of combining both photons and electron beams in the same plan. Anyway, a double divergence MLC model is recommended to minimize the scattering effect. On the other hand, a new electron MLC (eMLC) at the electron cut level could reduce the air scattering effect on the beam penumbra.

Material and Method: The analytical algorithms included in the treatment planning system are not reliable to calculate the delivered dose accurately for MERT. The optimization system used in this work is a home-made software based on the work by Jiang. The optimal intensity of profile for beamlets is calculated by COOKER home-made software using the Zangwill's penalty function method about the dose constraints and a gradient method to minimize the objective function. MCDOSE code is able to storage the dose deposition from every beamlet to each voxel in the CT of the patient. The bremsstrahlung leakage and electron scattering by the

MLC are not considered for the first step optimization, because the particles out of the field are not followed to simulate the dose contribution of one beamlet. In this work, we propose to solve 3-D real treatments following second optimization criteria by which multiple blocks (called blocklets) are generated from the leaf sequence to be treated as beamlets in order to re-weight the fields considering a realistic geometry for this second optimization step. The simulation of blocklets is less demanding regarding to required CPU time and the effect of electron scattering becomes no so severe.

Results: Dose volume histograms corresponding to the no optimized treatments versus the optimized ones by using re-weighted blocklets were compared. The lung and heart doses are always lower than 20 Gy and the best dose homogeneity on the target is achieved using the second-optimized plan.

Conclusions: An optimization procedure based on Monte Carlo was developed to calculate accurately the delivered dose using MERT. A Monte Carlo procedure is open to analyze the best geometry collimation by simulating commercial double focused MLC for photons or an electron MLC prototype. Other potential treatment sites like Head and Neck could be benefited of MERT.

189

Validation of a virtual electron beam head model for Monte Carlo dose calculation

M. Sikora, O. Dohm, S. Mika

Universitätsklinik für Radioonkologie Section for Biomedical Physics Tübingen, Germany

A virtual electron beam accelerator head model was developed and implemented into the fast XVMC Monte Carlo (MC) algorithm. The model employs parameterized analytical functions describing the properties of the particles generated by the treatment machine in a phase space plane, i.e. initial energy, position and direction. The phase space plane is located at the applicator end. The adjustment of parameters is performed by means of a fitting procedure applied to a set of measured data: depth dose curve and some cross-profiles in air to evaluate the fluence distribution and one depth dose curve in water to find the energy spectrum.

There are three main particle sources defined in the model: two Gaussian shaped point sources and a rectangular shaped area source. The Gaussian sources represent the primary electrons coming from the scattering foils. The area source models electrons scattered from the applicator. Also the photon contamination is evaluated from the measured data.

The model was validated by comparison of MC calculation results with the measured data for various geometrical setups - different applicator sizes and source to surface distances (SSD). The main aspects taken into account were accuracy of output factor and isodose distribution computations for open beams and beams modified by cut-outs. The accuracy of the model was shown in areas of large density inhomogeneities where hot or cold spots may occur. An improved gamma method was used to evaluate the agreement between the calculation results and the measured data. Deviation of calculated data was within 3 % for dose values and 2 mm for position of calculated points. A very good agreement was obtained between calculated and measured data in a homogeneous medium i.e. water and output factors were properly calculated with this model. Additional output factor calculation results were compared with values obtained with BEAMnrc. The MC code BEAMnrc is slower than XVMC, but it can be used as golden standard to evaluate clinically more practicable dose calculation algorithms.

190

Monte Carlo treatment planning of electron irradiation? early experiences

K. Nygaard, O. Odland, Y. Kvinnsland, L. Muren

Haukeland University Hospital, Dept of Oncology and Medical Physics, Bergen, Norway

Introduction: A Monte Carlo algorithm for electrons has recently become available in the Eclipse treatment planning system (eMC v. 7.2.34, Varian Medical Systems Inc., Palo

Alto, USA). Input-data to this algorithm consist of 1) depth dose curves for all electron energies and applicator sizes, 2) a profile and depth dose for a 40x40 cm² field without applicator and 3) absolute point dose measurement in the calibration depth for all energies and applicator sizes. Prior to clinical implementation, we performed additional measurements of profiles in open fields as well as 2D dose distributions below perspex edges.

Materials and method: The eMC algorithm is based on standard EGSnc Monte Carlo methods, but the electron transport through the patient is simplified and the number of electron transport steps is reduced, significantly reducing calculation times. In addition to the requested depth dose curves, dose profiles in 2 cm depth were measured in a water phantom for all electron energies and applicator sizes using an electron diode. Dose profiles in the same depth and depth dose curves were calculated using eMC and compared to the diode measurements. 2D dose distributions (depth and off-axis) below perspex edges of different thicknesses and angles were measured using a diode in the water phantom. Corresponding dose distributions below the same perspex edges were calculated using both the eMC algorithm in Eclipse and the Pencil Beam algorithm in Helax-TMS 6.1A (AB Nucletron, Uppsala, Sweden) and compared to the diode measurements. Comparisons were performed within the 20% isodose curve using the gamma-method [1] with acceptance limits of 3% in dose and 3 mm in position.

Results: The eMC algorithm showed good agreement with the diode measurements with clinically acceptable calculation times of 10-30 minutes, both concerning the profiles, depth dose curves and the 2D distributions. The agreement depended on the resolution and smoothing of the calculations. Single point deviations of as much as 6% were observed, mainly a result of statistical noise. For the 2D gamma-comparisons of the dose distributions below the perspex edges, 98% of the eMC vs. diode comparisons of the different field setups had agreement within the acceptance limits across more than 95% of the dose distribution. For corresponding comparisons between calculations using the Pencil Beam algorithm and diode measurements, 46% of the calculated dose distributions agreed with the diode measurements.

Conclusions: The eMC calculations of depth dose curves and dose profiles agreed with measurements performed in the water phantom. The eMC algorithm agreed with diode measurements far better than what the pencil beam algorithm did. Currently, eMC is being used for all CT-based treatment planning of electron irradiation at our institution.

1. Low DA, Harms WB, Mutic S, and Purdy JA. A technique for the quantitative evaluation of dose distributions. *Med Phys.* 25 (5): p. 656-61. 1998.

191

A finite size Pencil Beam algorithm for IMRT dose optimization based on Monte Carlo calculations

*U. Jelen, M. Söhn, M. Alber
Universitätsklinik für Radioonkologie, Section for Biomedical Physics, Tübingen, Germany*

One concept of IMRT assumes pre-computation of the dose as a superposition of small elements, called beamlets. Beamlet-based IMRT optimization imposes three main requirements for the dose pre-computation algorithm: 1) speed, due to a large number of beamlet dose distributions to be computed 2) simplicity of commissioning procedure, ideally based on broad beam measurements and 3) close proximity between optimized and the final dose recalculated with a high-precision algorithm, as a proper consideration of the dose gradients at every stage of optimization is crucial to assure fast convergence and realistic dose distribution.

A finite size pencil beam (fsPB) algorithm was designed and commissioned specifically for beamlet-based IMRT dose pre-computation. The algorithm employs an analytical function for the beamlet cross-profile - a finite size pencil beam kernel (fsPBK). The fsPBK shape is determined by means of a fitting procedure from broad beam dose distributions computed with XVMC Monte Carlo code. Its parameters are stored in look-up tables for a small set of field sizes and two energies (6

and 15 MV). To facilitate lateral and longitudinal density corrections the dependencies of those parameters on the density are derived in the commissioning procedure and used to appropriately rescale fsPBK like in convolution/superposition method. By choosing the size of the beamlets small enough arbitrary MLC fields can be created.

The algorithm was validated by comparison with Monte Carlo results in the virtual waterphantom showing satisfactory speed (thousands of beamlets per minute on a (3 mm)³ grid) and very good accuracy. The output factors of fields from 2x2 cm² to 20x20 cm² were computed with 2% precision. The accuracy of dose calculation was from 1-2% in water up to 5% in cases with severe inhomogeneities. Irregular, typical IMRT field shapes and segments were reproduced properly.

A fast pre-computation algorithm, based on a simple and small set of data, accounting for tissue inhomogeneities and enabling computation for arbitrary field shapes was developed. Accuracy of the algorithm was examined in phantom tests and for clinical cases requiring proper modelling of tissue inhomogeneities revealing very good agreement with Monte Carlo results. Implemented into the optimization scheme, the algorithm provides correct dose gradients and the density corrected dose distribution to be used at all steps of optimization, not only in the final, verification stage.

192

Calculating dose output at off-axis positions in photon beams using a laterally beam quality dependent pencil kernel model.

*J. Olofsson, T. Nyholm, A. Ahnesjö, M. Karlsson
Umeå University, Department of Radiation Sciences, Umeå, Sweden*

We have generalized a photon pencil kernel dose calculations model to include explicit modeling of off-axis softening (OAS). This is achieved by varying the kernel characteristics according to typical shifts in beam quality depending on the lateral position. The only measured input data needed for each individual photon beam is the quality index TPR_{20/10}. Calculations were made, both including and excluding the effect of OAS, and compared to measured results. Comparisons were performed at 5, 10, and 20 cm depth for four different photon beam qualities delivered by a Varian Clinac 2300C/D and a Siemens Primus accelerator. In total the dose was measured in 264 points located up to 18 cm from the central axis in a number of different fields of varying size and position. In all cases the results were normalised to the reference geometry for each beam quality, to reflect the absolute dose delivery per monitor unit (MU). Results that include the effect of OAS show significantly smaller deviations from measurements as compared to when it is excluded (improvements up to 5% were observed). In general the deviations including OAS are within ±1%, but some variations in the amplitude of the effect of OAS among the investigated beams seem to increase the deviations in some cases.

A pencil kernel model implemented to take lateral beam quality variations into account has the potential to significantly reduce systematic calculation errors at off-axis positions as compared to a standard implementation based solely on a central axis beam quality description.

193

Comparing analytical anisotropic and PBC algorithms against Monte Carlo dose calculations in an extreme water-lung interface

*I. Gagne, M. Hiltz, S. Zavgorodni
British Columbia Cancer Agency - Vancouver Island Centre, Physics Department, Victoria, Canada*

This study compares performance of the analytical anisotropic algorithm (AAA) to that of the single pencil beam convolution (PBC) algorithm in a vertical water-lung interface. Monte Carlo (MC) calculations that were previously benchmarked against experimental measurements¹ are used as a reference ("gold standard") in the comparison. The AAA algorithm is a 3D photon superposition/convolution dose calculation model newly implemented in the Eclipse™

Integrated Treatment Planning System (TPS). Earlier versions of this system use the PBC algorithm with the modified Batho inhomogeneity correction. The dose distributions were calculated at nominal beam energies of 6 MV and 18 MV, for $4 \times 4 \text{ cm}^2$ and $10 \times 10 \text{ cm}^2$ field sizes in a heterogeneous solid water-lung phantom geometry¹ using these algorithms. All calculations were performed with a $0.25 \times 0.25 \times 0.25 \text{ cm}^3$ grid size. Dose profiles at depths of 5, 10, and 15 cm were extracted and normalized at a depth of maximum dose with respect to the water-half of the phantom. A reduced chi-square test was applied to quantify the difference between the TPS and the MC derived data. The results showed that in all calculated cases the AAA algorithm provided lower chi-squared values than the PBC algorithm demonstrating that it models the heterogeneous phantom dose distribution more accurately. In the most difficult situation (18 MV energy, $4 \times 4 \text{ cm}^2$ field size), MC/TPS profile differences within the lung region were reduced from 15 % calculated with the PBC algorithm to 5 % with the AAA. These results demonstrate that the AAA algorithm is likely to perform with a clinically acceptable accuracy in realistic patient geometries, however further investigations are required to confirm this.

194

Monte Carlo calculations for arytenoid sparing irradiation of early stage vocal cord cancer

*S. van der Hout*¹, *B. De Smedt*², *N. Reynaert*², *P. Levendag*¹,
*B. Heijmen*¹

¹Erasmus MC, Radiotherapy, Rotterdam, The Netherlands

²Gent University, Medical Physics, Gent, Belgium

Routinely, early stage vocal cord cancers are irradiated with 2 lateral 6-MV photon beams with field sizes around $5 \times 5 \text{ cm}^2$. In this way, a relatively large volume of healthy tissue is also irradiated, leading to reduced voice quality as well as swallowing difficulties. In our institution, we are working on improved treatment techniques for these lesions, which should result in less side effects without reducing the local control rate. As a first step, for some of the patients the arythenoids can be blocked out of the fields, possibly resulting in improved swallowing possibilities. As a next step, suitable patients may be irradiated on a single vocal cord, potentially leading to improved voice quality.

With field size reduction, underdosage of the lesion, both due to lack of electron equilibrium at the tissue-air-interface as well as due to the field penumbras, will be more pronounced and ways to correct for that will have to be investigated and implemented clinically. In addition, patient setup must be very accurate, and lesion motion must be corrected for or taken into account.

The present study concentrates on dosimetry aspects. To determine the dosimetry in the vocal cord area, dose distributions calculated with our Pinnacle system were compared with Monte Carlo calculations (BEAMnrc), both for conventional treatment plans as well as for treatment plans with much smaller field sizes to block out the arytenoids. All experiments were performed at a Varian linac with a 6 MV photon beam. To get accurate results with Monte Carlo calculations, linac modelling calculations were compared with output measurements in a waterphantom. Output measurements were performed for different symmetric fields from 1×1 to $10 \times 10 \text{ cm}^2$ and for $2 \times 10 \text{ cm}^2$ offaxis fields, the results agree within 0.5% (1 SD). BEAMnrc and Pinnacle dose distributions will be presented and compared. Arytenoid sparing is possible, but clinically acceptable precision in predicted dose can only be obtained with Monte Carlo dose calculations.

195

Evaluation of the treatment planning system of the Cyberknife by means of a comparison to Monte Carlo calculation

*S. Cora*¹, *P. Francescon*¹, *C. Cavedon*¹, *M. Avanzo*¹, *J. Stancanella*¹, *P. Scalchi*¹, *E. Spezi*², *A. Ferri*², *C. Bergamini*²

¹Servizio di Fisica Sanitaria, "S.Bortolo" Hospital, Italy

²Servizio di Fisica Sanitaria, Policlinico S.Orsola-Malpighi,

Bologna, Italy

The goal of this work is the evaluation of the accuracy of the treatment planning system (TPS) of the Cyberknife, a frameless, robotic radiosurgery system, by comparing the dose distribution obtained by the TPS with the dose distribution calculated with a MonteCarlo code.

The frameless and non-isocentric operation of the CyberKnife makes it possible to utilize radiosurgery as a potential treatment throughout the body.

Unlike conventional TPS, the CyberKnife uses an inverse planning optimization process which allows the computer to determine the direction and weight of the beams.

Dose calculation in the Cyberknife TPS is performed by a simple numerical model which allows density scaling and oblique incidence to be taken into account, but does not correct for scattering from inhomogeneous media.

In this work, the dose distributions obtained for an extracranial treatment and a cerebral treatment have been compared with the dose distribution calculated with the BEAM and DOSXYZ Monte Carlo codes. Since the number of the beams to be simulated is very large (a complex tumor shape can require between 150 and 250 beams), the dose calculation has been performed remotely with the MARS (Multi Processor Array for Radiotherapy Services) cluster system. MARS is a 32 nodes Linux cluster implementing the openMosix kernel extension providing a total CPU power of 90 GHz. Radiotherapy plan settings, CT and VOIs were sent to MARS in the DICOM format and processed within the Matlab environment.

196

Upgrading of CAVRZnrc ionization chamber simulation code for accurate IMRT verification

*J. Pena*¹, *R. Capote-Noy*², *R. Linares*^{3,4}, *F. Sánchez-Doblado*^{3,4},
*F. Gómez*¹

¹Universidade de Santiago de Compostela, Particle physics, Santiago de Compostela, Spain

International Atomic Energy Agency, Nuclear Data Base, Vienna, Austria

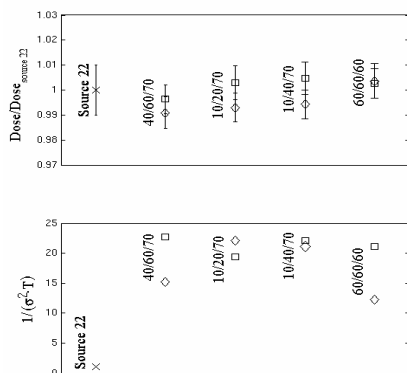
³Universidad de Sevilla, Fisiología Médica y Biofísica, Sevilla, Spain

⁴Dpto. Fisiología Médica y Biofísica, Facultad de Medicina, Universidad de Sevilla, Sevilla, Spain

Motivation: The purpose of this study is to present two improvements of the CAVRZnrc Monte Carlo code which include new geometries and accelerate the simulation of ionization chambers (IC) in reference and IMRT conditions.

Materials and methods: Available EGSnrc RZ user codes are designed to simulate plane-cylindrical geometries and can only simulate reference conditions for frontal incidence of radiation. Two new codes: CAVRZsphere and CAVRZcone, derived from the original CAVRZnrc user code, were developed to simulate spherical-ending and conical-ending cylindrical ion chambers, respectively. These new codes allow implementing reference conditions as defined in IAEA TRS-398 and TG-51 protocols for lateral incidence of radiation by the inclusion of a surface perpendicular to the Y axis that acts effectively as a phantom surface. A powerful variance reduction scheme was implemented, combining photon splitting on selected rectangular regions of the phase-space plane with a Russian roulette on a selected region of the phantom. This feature was specifically designed to boost those simulations where IC dimensions are small compared to the field dimensions or it is partially shadowed by the collimators, a very frequent situation in IMRT beamlets. The computation efficiency is increased up to 20-fold in comparison with standard EGSnrc RZ ISOURC=22 simulations.

Results:



Caption: dose and efficiencies obtained in the calculation of the dose scored in a 0.1 cm³ water volume in the centre of a 10cm x 10cm field at 1 cm in-water depth for different combinations of splitting parameters (a/b/c) and with RR switched ON (□) and OFF (◇) compared to that obtained with the standard ISOURC = 22 source.

Conclusions: These two new codes allow the Monte Carlo simulation of IC whose geometry couldn't be reproduced with the currently available codes. Due to the new variance reduction techniques included in these two new codes, computation times are drastically reduced.

IMRT (combined)

197

Influence of the linac design on IMRT

R. Topolnjak¹, U. van der Heide¹, C. Raaijmakers¹, G. Meijer²
¹University Medical Center Utrecht, Department of Radiotherapy, Utrecht, The Netherlands
²Catharina Hospital Eindhoven, Department of Radiotherapy, Eindhoven, The Netherlands

The purpose of this study is to characterize the impact of four parameters in the design of a linac on IMRT treatment plans. These parameters are 1) leaf thickness, 2) source size and the distance source-MLC-patient, 3) MLC leaf width 4) the number of the gantry angles that can be used realistically. The parameters can be influenced by changing transmission, penumbra, leaf width and the number of the beams in the treatment planning program.

Three head-and-neck patients with stage T1-2N1-2 oropharyngeal cancer were observed and for each patient ten plans were made. For the primary tumor and the positive lymph nodes the prescribed dose to the GTVs was 69 Gy and for the CTVs 66 Gy. The prescribed dose for the elective lymph nodes was 54 Gy. Organs at risk (OAR) were the parotid glands, the spinal cord and the body. The requirements are challenging because of the variation in target dose and the overlap of targets with OARs. Therefore, sharp dose gradients are important. In order to compare plans, hard constraints were imposed on the target coverage: 99% of the target volume has to receive at least 95% of the prescribed dose. In addition the OARs must be spared as much as possible. For each plan in our investigation only one linac parameter was modified while others were set to default values: transmission 1.5%, penumbra 5mm, leaf width 10mm and 7 beam angles.

Before varying the linac parameters, the clinical plans were re-optimized. By pushing constraints on the dose to OARs, better sparing of the left [LP] and the right parotid [RP] glands was achieved

| | Transmission [%] | | | Penumbra [mm] | | | Leaf width [mm] | | Number of beams | |
|---------|------------------|------|------|---------------|------|------|-----------------|------|-----------------|------|
| | 5 | 1.5 | 0.1 | 10 | 5 | 1 | 10 | 5 | 24 | 7 |
| LP[Gy] | 23.6 | 15.1 | 13.3 | 15.4 | 14.1 | 13.6 | 14.1 | 13.8 | 12.3 | 14.1 |
| RP [Gy] | 35.3 | 28.6 | 27.7 | 28.8 | 26.9 | 26.8 | 26.9 | 25.1 | 25.9 | 26.9 |

The plans obtained for different values of transmission were similar in number of segments and efficiency. The decrease of transmission through the leaves substantially decreases the dose to the parotid glands. Varying the penumbra gives the same, but less strong effect. Finally, the dose to the parotid glands decreases when using either leaves of smaller width or bigger number of beams, but with the drawback of increasing the number of segments. Here, we note that results for 5mm leaf with and 24 beams could further improve by using a transmission smaller than 1.5%. In conclusion, optimization of each of the four parameters result in a slight improvement of the IMRT plans in term of OARs sparing.

We acknowledge Elekta for their support.

198

IMRT using the new variable aperture collimator

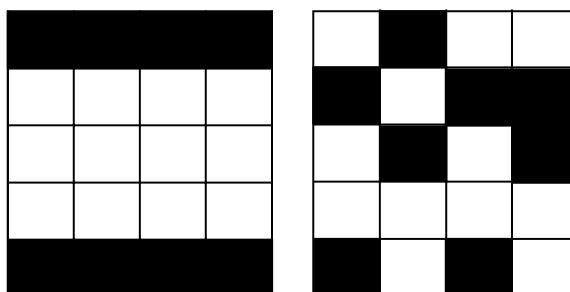
J.W. Anderson¹, G. Echner², C. Lang², R. Symonds-Taylor¹, G. Hartmann², W. Schlegel², S. Webb¹
¹The Institute of Cancer Research, Joint Department of Physics, Sutton, UK
²German Cancer Research Center (DKFZ), Medical Physics, Heidelberg, Germany

Purpose: To design and construct a variable aperture collimator (VAC) and investigate its ability to deliver highly irregular fluence patterns. These patterns include isolated "islands" of low dose formed using single bixel attenuators (SBAs).

Method: The VAC was constructed in cooperation with DKFZ in Heidelberg. It consists of four columns, each with two single-bixel attenuators that can each be moved to any position within that column. Each SBA moves in a focussed arc and is itself doubly focussed to produce a one square centimetre low-dose shadow at the isocenter.

Results: Preliminary dosimetric analysis of the VAC prototype has shown that a single SBA in an open field produces a low dose region with minimum transmission of 11.6% and a full width at half maximum of 10.5mm.

Conclusion: The results acquired to date indicate that the VAC is capable of directly producing the highly irregular field shapes required by intricate IMRT. This presentation will detail precisely what can be achieved with the VAC, both in terms of a single irregular field and the sum of multiple static fields.



Two possible VAC configurations. White squares are open and dark squares are attenuating SBAs.

199

An IMRT adaptation concept for interfractional organ motion

K. Bratengeier
 University of Würzburg, Strahlentherapie, Würzburg, Germany

Intensity modulated radiotherapy (IMRT) is more sensitive to interfractional motion than conventional tumour conforming techniques. Ad-hoc adaptation to the daily target and OAR positions (OAR: organ at risk) has to be performed very quickly. The daily IMRT optimization process has to be

carried out in a certain time frame and the resulting plan should resemble the original one as close as possible. Therefore a time consuming verification of the new plan can be minimized. The aim of this work was to propose a fast method for daily IMRT-plan adaptation.

The method is based on geometrical considerations. It is an extension of an optimization method referred as 2-Step IMRT. For this approach the radius of the OAR and its distance to the target volume (TV) as well as the diameter of the TV are relevant. It is shown that in most cases only two intensity levels (steps) are necessary to compensate "shielding" effects of the OAR. All parts of the TV except the OAR, which is to be blocked out, define the first dose level which corresponds to the first segment of any field. The second segment is placed tangentially to the OAR. Its width depends mainly on the gap width between the OAR and the TV. In many cases this additional segment is much smaller than the first one and it is only a little bit broader than the gap. The most important value is the width-weight-product of the additional segment. This is, generalized, the integral over the aperture of the additional segment.

Examples demonstrate that 2-Step IMRT only needs few segments, however, more gantry angles than usual IMRT-techniques. It can be shown that 2-Step IMAT is relatively insensitive to intrafractional organ motion. The rules to create a 2-Step IMRT plan can also be used to adapt a plan to the daily target position. For adaptation of any preplanned IMRT-plan it is proposed to identify the segments linked to the blocking-out-compensation of the OAR and then to apply the adaptation rules.

200

Quantification of differences between planned and delivered IMRT dose distributions in terms of complication-free tumor cure

P. Mavroidis², B. Costa Ferreira¹, R. Svensson¹, K.

Theodorou², B. Lind¹, A. Brahme¹

¹Karolinska Institutet, Dept Med Rad Phys, Stockholm, Sweden

²Larissa University Hospital, Dept Med Physics, Larissa, Greece

Background: Intensity modulated radiation therapy is today performed with such a conformity to internal target volume in the patient that even a small misalignment between the incident beams and the target can dramatically reduce the effectiveness of the treatment. Consequently, there is a need for a measure that could quantify the accuracy of a delivered treatment in terms of expected clinical outcome.

Material and Methods: To evaluate such a measure, a cervix cancer was selected as the tumor site on the grounds that the involved organs at risk, mainly the bladder and the rectum, are very close to the tumor and partly located inside the internal target volume. A treatment plan delivering a conformal dose distribution was designed using the anatomy of the phantom. The phantom, with films positioned into it, was irradiated. The dose distribution delivered was derived from the film and compared with the one of the treatment plan.

Results: The results were evaluated using both physical and biological criteria. The main purpose of this parallel evaluation was to compare the values of physical and biological evaluations in quantifying the accuracy of treatment delivery. It is shown, that the physical comparison of the dose distributions do not generally express their real difference in treatment effectiveness. It is demonstrated how small inaccuracies in dose delivery can considerably deteriorate a conformal treatment plan.

Conclusions: The clinicians need to know how much the expected complication and control rates will increase and decrease respectively because of uncertainties in dose delivery. In conformal IMRT delivery, the reliability of the patient setup procedure becomes critical for the effectiveness of the treatment.

201

Improvement of the accuracy of EPID lung image analysis validated with Cone Beam CT

M. Buijs, M. Van Herk, A. Betgen, J. Sonke

The Netherlands Cancer Institute, Radiotherapy, Amsterdam, The Netherlands

Purpose: Since early 2004 a kilo voltage Cone Beam CT (CBCT) guided linear accelerator is in clinical use at the NKI-AvL. As part of our acceptance procedure, setup errors determined with our EPID system were compared with data of the CBCT system on bony anatomy. These tests showed good results for prostate and head and neck, but demonstrated that EPID image analysis of lung patients was inaccurate. The EPID underestimates the setup error, particular in the AP direction. The aim of this study is to improve the accuracy of EPID imaging analysis by developing, testing and implementing new tools for setup measurement validated with CBCT data.

Method: Clinically, setup error was measured by 3D CBCT-to-planning CT matching. Our standard EPID image analysis procedure is a manual DRR template-to-EPID match. As an alternative to improve the accuracy, we evaluated of unsharp mask enhanced DRR-to-portal image manual matching in one window. Both EPID analysis methods were tested on 86 AP and 86 lateral images of ten lung cancer patients. Differences between quantified relative to the clinical CBCT registration.

Results: The difference between the standard EPID image analysis procedure and CBCT was 2.4, 2.3, 2.2 mm (1 SD) in the left-right, cranial-caudal en anterior-posterior direction. Using unsharp masked window manual matching this difference is reduced to 1.9, 1.5 and 1.7 mm. The slope of the set up error measured with CBCT and the EPID analysis was determined for both methods. For the standard EPID analysis the slope was 0.8 for LR, 0.8 for CC and 0.25 for AP. For the unsharp mask enhanced windows match, the result improved to 1.01 (0.91-1.11 95% CI) for LR, 0.88 (0.79-0.96 95% CI) for CC and 0.73 (0.60-0.85 95% CI) for AP.

Conclusion: New tools for image analysis improve the match accuracy of the EPID image analysis for lung set up measurement as validated with CBCT. However there is still an underestimation of the set up error measured with these tools in comparison with the measured set up error with CBCT. Therefore, we will evaluate different enhancement filters and automatic grey value registration in the near future.

202

Simultaneous Integrated Multi-target Treatment with IMRT for tonsil tumours. Comparison with 3DCRT combined with brachytherapy

A. Bäck¹, C. Mercke², K. Johansson¹

¹Göteborg University, Radiation physics, Göteborg, Sweden

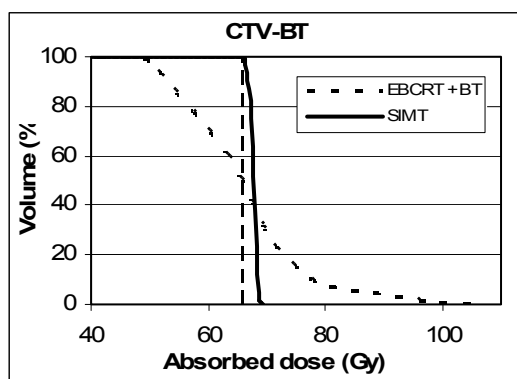
²Göteborg University, Radiation oncology, Göteborg, Sweden

Introduction: A great deal of experience with radiation therapy of head and neck cancers has demonstrated the need of a high absorbed dose to maximise the probability for local control and thereby cure. Our centre has long experience of combined induction chemotherapy, external beam conformal radiotherapy (EBCRT) and brachytherapy (BT) for tonsil cancer patients with good results regarding tumour control. However, the frequency of complications for these patients is high with, for example, xerostomia and in some patients tissue necrosis. A planning study with the purpose to evaluate the impact of the dose distribution of IMRT treatment of tonsillar carcinoma using a simultaneous integrated multi-target treatment (SIMT) is performed. The objective is to investigate the possibilities of replacing a combined EBCRT treatment and BT treatment with one single IMRT session. The goal is to retain the good local tumour control and reduce complications by reducing the dose to healthy tissue, specifically the parotid glands and the minor salivary glands in the oral cavity, the mandible and other critical tissues.

Material and methods: The Helios inverse planning system included in Eclipse dose planning system was used to create SIMT dose plans for four tonsil cancer patients with tumours

in different stages. Target volumes and organs at risk were delineated and new fractionation schedules were designed using isoeffective dose calculations. The overall treatment time was reduced with SIMT. The treatment plans were prepared for dynamic MLC delivery. The IMRT dose plans were compared to the combination of EBCRT and BT treatment actually used for those patients.

Results and discussion: It was found that the SIMT technique reduced the expected frequencies of complications in several critical organs, for example parotid glands, mandibles and oral cavity. The same isoeffective doses was given to the target volumes with increased dose homogeneity compared to the doses created in a combination of EBCRT and BT. The dose distribution in the target volume (CTV-BT) treated with BT in the original plan will appear significantly different for the different techniques, see figure (the dotted line indicates the prescribed dose). Furthermore, the SIMT technique makes it possible to define this target volume more freely without the limitations enclosed by the BT technique and thereby optimise the treatment. A clinical study is, of course, needed to confirm the theoretical results and to evaluate whether there will be any differences in tumour control because of the changed dose distribution in CTV-BT.



203

A concomitant tumour boost in bladder irradiation: Patient suitability and the potential of intensity-modulated radiotherapy

L. Muren¹, A. Redpath², D. McLaren³, J. Rørvik⁴, O.

Halvorsen⁴, J. Høstmark⁵, A. Bakke⁵, T. Thwaites², O. Dahl¹
¹Haukeland University Hospital, Dept of Oncology and Medical Physics, Bergen, Norway

²Western General Hospital, Dept of Oncology Physics, Edinburgh, UK

³Western General Hospital, Dept of Radiation Oncology, Edinburgh, UK

⁴Haukeland University Hospital, Dept of Radiology, Bergen, Norway

⁵Haukeland University Hospital, Dept of Urology, Bergen, Norway

Background and Purpose: Dose escalation without increased intestinal and urinary adverse effects is a main goal in radiotherapy (RT) of urinary bladder cancer (UBC), and might be achieved with a concomitant bladder tumour boost. In this study we quantified 1) the fraction of patients suitable for such a boost, and 2) the potential of intensity-modulated RT (IMRT) to achieve it. Due to the documented bladder motion, the IMRT planning was performed with two margin alternatives.

Material and Methods: The fraction of patients suitable for a boost was quantified using two patient series, one consisting of 30 presumed radical therapy candidates, one of 15 consecutive RT patients. The IMRT planning was performed using the latter RT series. Two sets of targets were created for the patients suitable for a boost, using i) wide and ii) narrow margins around both the tumour and the bladder. IMRT plans with 3, 5, 7 and 9 equi-spaced dynamic

beams were set up, and a 20% concomitant boost was prescribed to the tumour with margins. The optimisation minimised the quadratic dose deviation across both targets whilst fulfilling dose-volume histogram (DVH) constraints for the intestine, rectum and the normal tissue outside the targets (NT). The constraints were based on corresponding results for 3- and 4-field conformal RT (CRT) plans, and iteratively reduced while ensuring adequate target coverage (at least 99.5% of the target receiving >95% of the prescription dose (PD)).

Results: Thirteen of the 30 radical therapy candidates (43%) and 10 of the 15 RT patients (67%) were suitable for a boost. The 20% boost could be obtained while maintaining target coverage with at least one IMRT plan in 9 of 10 cases with wide margins and for all 10 cases with narrow margins. Using wide margins, all 3-field plans were unacceptable, the 5-field plans were acceptable for 5 of 10, and the 7- and 9-field plans for 9 of the 10 patients. With wide margins, the volumes of intestine, rectum and NT receiving doses > 100% of the PD were on average reduced by a factor of 3-4 compared to CRT, e.g. for the intestine, from 78 cm³ to 24 cm³. The normal tissue volumes receiving intermediate doses (73-88%) decreased slightly, whereas volumes receiving the lowest doses (30-48%) increased, most pronounced for the NT. No striking differences were found between the 5-, 7- and 9-field plans, except for an increase in the volume of NT receiving doses > 30% of PD. The plans with narrow margins showed similar trends, but resulted in markedly lower normal tissue irradiation.

Conclusion: A considerable proportion of primary UBC patients were suitable for a tumour boost. IMRT allowed for the delivery of a 20% concomitant bladder tumour boost while both maintaining target coverage and reducing the normal tissue volumes receiving high doses. A 7-field set-up is required to obtain acceptable target coverage in the majority of patients with the currently accepted margins. The IMRT planning outcome using narrow margins (with very low normal tissue irradiation) showed great potential for further improvement of the treatment of this disease by using image-guided RT.

204

Is there a role for radiation therapists in the delineation of organs-at-risk in conformal radiotherapy for prostate cancer?

K. Fitzpatrick, C. Kelly, P. Thirion

St. Luke's Hospital, Clinical Trials Unit, Dublin, Ireland

Background: In Europe, physicians are usually in-charge of the organ-at-risk (OAR) delineation in the conformal radiotherapy planning process. As part of a research study, a radiation therapist (RT) was asked to delineate different OAR for 3-Dimensional Conformal Radiation Therapy (3DCRT) for localised prostate cancer.

Materials and Methods: 210 patients diagnosed with localised intermediate/high-risk prostate cancer were included in a phase III randomised trial [St. Luke's Hospital, 06/1996 to 12/2001] comparing two durations of hormonal blockage in combination with 3DCRT (70Gy/35 fractions). Radio-induced acute and long-term toxicity data was prospectively recorded. The present ongoing study is a retrospective analysis aiming to correlate various dosimetric parameters and toxicity events, specifically looking at the impact of different OAR designs: 1/ Rectum: Whole rectum from recto-sigmoid junction to anorectal junction vs 1cms above and below the PTV, and outer rectal delineation vs. rectal wall; 2/ Bladder: Outer bladder delineation vs. bladder wall delineation; 3/ Bladder and rectum PRV (0.5 to 1 cm expansion); 4/ Femoral Heads: Femoral head only vs. femoral upper third (down to lesser trochanter).

Results: A fully qualified RT is employed on a part-time basis for the study since June 2004. Over a period of 8 weeks, training on the use of the TPS (Helax-TMS-Nucletron v. 6.0) and on radiology-based anatomy was conducted under the supervision of a principal physicist and a senior radiation oncologist (RO) respectively, using academic publications and practical case studies. The RT delineated 20 test cases under close supervision and in September 2004 the training was considered complete. Since then, an average

of 15-20 plans per week are re-designed with a total of 150 individual plans completed to date. As part of the study protocol, all plans are checked by an RO and the number of OAR modifications are prospectively recorded. Based on a sample of 39 plans, the estimated median duration for plan re-design was 50 min (45 to 70). The correction per OAR per slice (0.5 cm slice) were as follows:

| OAR | Mean | Min | Max |
|-------------------------------|------|-----|-----|
| Rectum | 3.20 | 0 | 10 |
| Bladder | 2.95 | 0 | 12 |
| R Femoral | 1.8 | 0 | 5 |
| L Femoral | 2 | 0 | 4 |
| Total correction /plan | 9 | 0 | 21 |

No time trend was demonstrated.

Conclusions: Following proper training, OAR delineation can be successfully achieved by an RT. The persisting modification rate observed seems to be mostly in relation to the inherent inter-observer variation in CT scan-based OAR delineation.

Wednesday, September 28, 2005 Symposia

IMRT

205

Optimization of IMRT

M. Alber

Universitätsklinikum Tübingen, Germany

By its very nature, the IMRT optimization problem is governed by contradicting and mutually exclusive goals. Target coverage and normal tissue sparing, delivery time, treatment machine limitations and the laws of physics need to be reconciled to obtain a treatment plan which is by necessity not optimum in all aspects. For this reason, some order needs to be imposed on these goals to formulate a comprehensive set of rules according to which the optimization algorithm can make its decisions.

The most widely employed ordering is by importance weights for target and normal tissue goals. Its drawback lies in the fact that the various importance weights interact and do usually not control the goals in an intuitive manner. Closely related to importance weights is the concept of Pareto optimality, which seeks points where none of the goals can be improved further without compromising any other goal.

Of greater practical utility are approaches which treat a subset of goals as hard constraints. In this manner, the strong interaction between goals can be controlled, and even quantified by a sensitivity analysis. Constrained optimization approaches can be enhanced by lexicographic ordering, which is a multi-layered approach where the number of fixed constraints increases in each layer. Alternatively, constrained optimization can be combined with multi-criteria approaches. In any case, it is necessary to include both the MLC-sequencer and the final dose computation algorithm into the optimization lest the optimization result is spoiled by the post-processing of the fluence distributions. Given this level of integration, it is usually possible to formulate class solutions for many case classes, and obtain treatment plans whose delivery time is close to the theoretical efficiency limit.

206

Guidelines for the verification of IMRT. Report of an ESTRO working group

B. Mijnheer

The Netherlands Cancer Institute, Amsterdam, The Netherlands

Acceptance testing and systematic QA of planning and delivery of IMRT are different procedures compared with corresponding actions for other conformal RT techniques. The special hard- and software necessary for the planning and delivery of IMRT is rather complex while the vendors continuously offer improvements of their systems. With respect to the acceptance testing of IMRT delivery systems, high demands are made upon leaf position accuracy, linac performance for small number of MU delivery, the control system for leaf movement, and leaf speed stability. The treatment planning system requires a thorough insight in the factors determining the accuracy of the dose calculation such as the transmission and leakage through the leaves, the tongue-and-groove effect, the description of the penumbra and the dose outside the high-dose region. Furthermore the accuracy of the calculation of the dose in small fields and the effects of grid size on dose calculation and display should be known. Also the uncertainties in volume and dose-volume histogram determinations have to be assessed.

In recent years both the hard- and software became more mature, while also more experience with respect to QA of IMRT became available. As a consequence many more institutions, also smaller and busy clinics, started with IMRT, facing the problem of performing a comprehensive QA programme in routine clinical practice. For these reasons ESTRO is preparing a report dedicated to the verification of IMRT. In this report the various approaches for IMRT verification and the methods of data analysis are described. Ideally the actual dose delivery, in three dimensions, of patient treatments should be verified after performing a comprehensive QA programme of the various separate phases of the planning and delivery process of an IMRT

treatment. At this moment *in vivo* dose verification of IMRT is only employed in a few institutions, and pre-treatment verification of IMRT delivery, applying a large variety of phantom-detector combinations, is therefore used instead. After comparing the various techniques for dosimetric verification, the separate dosimetry/phantom systems are discussed in more detail. The report then summarizes QA tests for accelerator and MLC performance. In a separate chapter the use of independent dose calculations, including Monte Carlo computations, for IMRT verification is discussed. Various examples are given of patient specific QA procedures. The report ends with formulating guidelines concerning type, frequency and tolerances of tests to be performed for IMRT verification in relation to the required accuracy.

207

First clinical experiments with image and dose guided radiotherapy

B. Hesse, S. Nill, T. Tücking, U. Oelfke

DKFZ, Medical Physics, Heidelberg, Germany

Purpose: Conventional radiation therapy assumes that possible movements of organs during therapy can either be neglected or taken into account in the planning phase. Recently, we introduced a novel hardware design to overcome this limitation. An in-line cone-beam CT was integrated on a Siemens linear accelerator providing a radiographic localisation of bone and soft-tissue targets and an on-line *in vivo* 3D reconstruction of delivered dose. The purpose of this paper is to present our first clinical experience with this system in image and dose guidance.

Methods: Anatomical images of the patient in treatment position and a 2D beam monitor are required for an image and dose guidance in radiation therapy. 3D CT volume imaging were performed with the in-line cone-beam CT system where a kV X-ray tube is integrated with a SIEMENS Primus linear accelerator in-line but opposite to the therapy source and a flat-panel detector RID1640 (Perkin Elmer) is mounted at the Linac head, in front of the patient. Cone-beam CT scans were made of 5 Patients with prostate and head and neck cancer. For all 6 Patients the treatment beams were recorded during IMRT treatment beam delivery with the flat-panel imager by acquiring sequences of beam segment images. Each image was deconvolved to 2D input fluence distribution using an empirically derived scatter kernel and summed resulting in a corresponding 2D input fluence distribution. The resulting 3D dose distribution was then calculated based on planning CT by importing these measured input fluence matrices into the planing system. For the 2 head and neck cases the measured dose distribution was also calculated and reconstructed based on the on-line CBCT.

Results: A very good agreement could be seen between planned and reconstructed dose distributions. The error was calculated to be less than $\pm 3\%$. An error of less than ± 3 mm was seen for isodose lines down to the 50% line.

Considering some observed interfractional set-up errors also the agreement for the on-line CBCT based dose reconstruction is in the same order.

Conclusion: Our clinical validation showed that with the integrated in-line CBCT system interfractional set-up errors could be observed based on bony anatomy. For dose guided radiotherapy, the method of entrance dosimetry was developed. Generally good agreement was seen between planning, reconstruction and direct measurement of fluence and three-dimensional dose distribution.

208

Margin-less prostate IMRT plans, directly optimised for TCP including geometrical uncertainties

M. Witte¹, J. van der Geer¹, C. Schneider¹, J. Lebesque¹, M.

Alber², M. van Herk¹

¹*The Netherlands Cancer Institute - Antoni van Leeuwenhoek hospital, Radiotherapy, Amsterdam, The Netherlands*

²*Uniklinik fuer Radioonkologie, Radiooncolog, Tuebingen,*

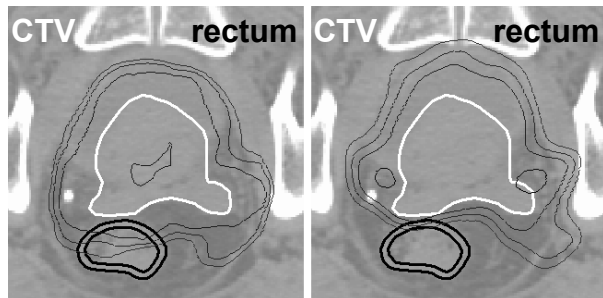
Germany

Purpose: To account for geometrical uncertainties without the use of margins during IMRT planning such that optimal values are obtained for the population averaged TCP and NTCP functions.

Methods and materials: A new method of computing cost functions was implemented within the inverse treatment planning tool Hyperion. This method optimises population-averaged values of implemented cost functions (e.g. EUD_{pop}, (N)TCP_{pop}), simulating random errors by blurring the dose, and systematic errors by displacing target and OAR volumes relative to the dose distribution.

Prostate plans (including seminal vesicles) for a five beam setup were created, optimising TCP_{pop} while constraining rectum EUD_{pop} and the maximum dose to the target. Gaussian distributions were used for the systematic and random errors (translations only, no attempt was made to realistically model organ motion for the rectum). Since geometric uncertainties were accounted for within the cost functions, no CTV to PTV margin was required. For comparison, conventional plans were created using the Simultaneous Integrated Boost (SIB) technique (68Gy to PTV with 1cm margin, 78Gy to boost PTV with 5mm margin except 0mm towards rectum). The resulting dose distributions were evaluated using an independent treatment plan evaluation tool that simulates the effects of geometric uncertainties.

Results: Compared to SIB the proposed optimisation technique reduced the dose delivered to the rectum, while expanding the high dose region in other directions (see Fig. 1). Rectum NTCP_{pop} could be reduced by as much as 50% (depending on patient geometry) while maintaining TCP_{pop}.



Due to an increased computational burden this method roughly doubles optimisation times, compared to SIB. However, a reduction of free optimisation parameters simplifies the optimisation process, and no (boost-) PTV's need to be created.

Conclusions: The computation of TCP and EUD including knowledge of geometric uncertainties within the inverse IMRT optimisation loop is feasible, and results in robust prostate treatment plans with an improved balance between local control and rectum toxicity, compared to conventional techniques.

Image guided radiotherapy

209

Geometric and Dosimetric Gains from IGRT

G.T.Y. Chen, Ph.D., J. Hawthorne, J.A. Wolfgang
Department of Radiation Oncology, Massachusetts General Hospital and, Harvard Medical School, Boston MA

Improved geometric accuracy through image guided therapy in radiation treatment delivery can reduce normal tissue irradiated. This may lead to a potential dosimetric gain to normal tissue. One approach to assessing this gain is to examine specific cases and build experience in which motion mitigation strategy should be applied.

How large is the dosimetric gain from various motion mitigation strategies such as gating, tracking, or treating the ITV, and how do they change as a function of tumor size, location, and motion amplitude? Such calculations can be a tedious and time consuming to perform. With the advent of

4D CT, we are faced with up to 10 times as much CT data, with a corresponding increase in the tasks of image segmentation and multiple dose calculations. We have recently investigated the utility of computational phantoms to aid in understanding dosimetric gains from IGRT. The phantom used is NCAT, developed by Segars(1). This phantom can be scaled and anatomical model parameters set to approximate aspects of patient 4D CT scans. The program generates 4D CT studies, complete with 4D organ contours and voxel displacement maps. Code has been written to calculate the volume of normal tissues irradiated, with the additional flexibility that tumor size, shape, location, motion amplitude and periodicity can be set by an input parameter file. By calculating the volume of normal tissue irradiated in a controlled phantom, we can estimate the benefits and gains from gated or tracked treatment as a function of tumor parameters. The generated CT data can also be used as input into dose calculation engines, to generate estimates of DVHs under various treatment scenarios. Initial analysis with the computational phantom shows that there is marginal gain in tracking vs. gated treatment. The volume of normal lung irradiated is a function of the tumor radius and amplitude of motion. Details of the analysis will be presented.

(1) WP Segars: [Development and Application of the New Dynamic NURBS-based Cardiac-Torso \(NCAT\) Phantom](#), Ph.D. Dissertation, The University of North Carolina, 2001.

210

Radiotherapy of prostate cancer guided by dynamic MRI and MRS

L.P. van der Vigt¹, J.J. Fütterer², E.N.J.Th. van Lin¹, A.L. Hoffmann¹, P.J.M. van Kollenburg¹, J.A. Witjes³, J.O. Barentsz², A.G. Visser¹

University Medical Centre Nijmegen, Departments of ¹Radiation Oncology, ²Radiology and ³Urology, Nijmegen, The Netherlands.

Purpose: To demonstrate the feasibility of the fusion of functional MR imaging techniques with CT using gold markers as fiducials, for image registration and to define the biological target volume for high-dose dominant intra-prostatic lesion (DIL) boosting with IMRT.

Method: Four fine gold markers (1x7 mm) were inserted under trans-rectal ultrasound guidance in patients with localized prostate cancer. Patients (n=7) underwent both CT and MR imaging on the same day, at least one week after implantation of the gold markers.

The planning CT scan was obtained at 3-mm slice thickness using an endorectal balloon. MR imaging with a similar endorectal balloon, was performed obtaining T2-weighted, spectroscopic and dynamic contrast-enhanced MR imaging. The gold markers were well visible on both CT and MR imaging sets. The CT and MR images were aligned by registration of the gold markers, by using an interactive closest point surface matching technique.

The T2-weighted MR was used to define the prostate anatomy, as a tool for prostate gland delineation. The functional MR data were used to define the DIL. An experienced radiologist and radiation oncologist reviewed all the data. For each patient two IMRT plans were compared: the DIL-IMRT plan, with the whole prostate to 70 Gy and the DIL to 90 Gy, and an IMRT-78 plan where the whole prostate was treated to 78 Gy.

Results: The datasets could be registered with a precision of 1.1 mm. The whole imaging procedure, CT-MR fusion and DIL-IMRT treatment planning could be performed within one day. In all patients, the combination of spectroscopic and dynamic contrast-enhanced MR yielded a clearly defined DIL volume (ranging from 1.1 to 8.5 cc). The dose distribution of the inner rectal wall circumference for the DIL-IMRT plans showed clearly a decrease of dose exposure to the rectal wall mucosa, resulting in decreased expected rectal toxicity, as compared to the IMRT-78. The estimated prostate tumor control was comparable.

Conclusion: Precise alignment of MR and CT images of the prostate is feasible using implanted fiducial gold markers, an endorectal balloon and a dedicated image registration method. Functional MR imaging can be used to define the DIL

for boosting with IMRT. Preliminary data suggest a decrease in late rectal toxicity with the DIL-IMRT plan.

211

Clinical introduction of image-guided radiotherapy, IGRT with Cone Beam CT

B. Sorcini, R. Odh, P. Näfstadius, I. Näslund, P. Wersäll, A. Tilikidis, A.C. Severin, A. Isoz, P. Fjällman
Karolinska University Hospital, Stockholm, Sweden

Introduction: The Cone-Beam CT, CBCT systems provides the capacity for soft-tissue and volumetric imaging of the patient in the treatment position, and are very useful for on-line repositioning during treatment delivery. The linear accelerator with On-board imager, OBI provides this opportunity and it focuses on localizing tumors based on internal anatomy, not just on the conventional external marks or tattoos.

Methods and Materials: The CBCT is clinically in use at the Karolinska University Hospital from beginning of March 2005. The CBCT is particularly important for us in the context of Extracranial Stereotactic Radiation Therapy, ESRT, where small targets treated to very high doses (15-45 Gy) in few irradiation fractions (1-3). The quality of the image for clinical use is adequate for target and soft tissue structures differentiation such as bladder and rectum. The CBCT software is intergraded with treatment console and we using currently the manual online registrations tools for our clinical set-up correction protocol.

Results: Using the 3D manual image registration, a match between the planning scan and verification CBCT scan was achieved and verified using the split view. This gave a good correlation between the two data sets. The dose to patient during CT acquisition is about 3 cGy for full fan geometry and 5 cGy for half fan geometry. An example of a successful registration of prostate is shown in Fig 1. The on-line 3D treatment set-up verification require about 7 minutes extra time due to acquisition, reconstruction and 3D registration.

Conclusions: The use of image guided radiotherapy will provide greater confidence of both conformal targeting and avoidance, whether this is carried out prior to treatment or on the treatment unit may depend on time constraints within departments. The initial experience of CBCT is very encouraging with the image quality adequate for internal soft target localization. The workloads generated by set-up correction in relation to their benefits have to be considered.

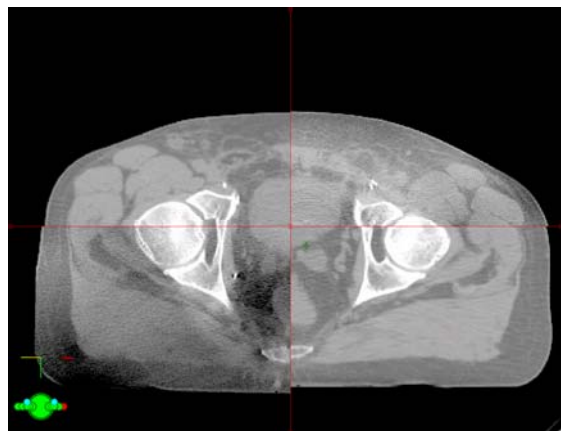


Figure 1: Image registration of planned CT (GE high speed 16) and Varian CBCT - prostate (CBCT - top right, bottom left)

Patient positioning in RT

212

Experience with the Novalis system

M. Mast, C. Niël, J. van Santvoort, J. van Egmond
Haaglanden Medical Centre Location Westeinde Hospital, Den Haag, The Netherlands

Introduction: In radiotherapy sparing of critical structures and normal tissue is essential to reduce toxicity and morbidity. With stereotactic radiotherapy (fractionated) and radiosurgery (single fraction) accurate fixation of the patients in combination with highly conformal beam shaping by the use of a micromultileaf collimator is feasible, hence a decrease of the CTV-PTV margins can be obtained. Smaller margins result in lower dose in the normal tissue in the near proximity to the target volume. Stereotactic treatment results in rapid falloff in the radiation dose and precise focal dose delivery. Precise patient positioning and position verification is essential in this form of radiotherapy. We evaluated this on our Novalis.

Materials & methods: We started patient treatment with intracranial tumours on a Novalis accelerator in June 2004. Head fixation was performed by a relocatable stereotactic frame and a standardised upper jaw fixation (BrainLAB). Positioning errors were determined with the Exactrac X-ray 6D system to assess the inter-fractional accuracy of patient positioning in the BrainLab mask system till now in 9 patients (a total of 68 fractions). We also evaluated the intra-fraction movement on 3 patients (a total of 19 fractions).

Results:

For the inter-fraction positioning errors:

| | Translations (mm) | | | Rotations (degrees) | | |
|----------------------|-------------------------|-------------------------|-------------------------|--------------------------|--------------------------|--------------------------|
| | Vertical | Longitudinal | Lateral | Table | Longitudinal | Lateral |
| Average (min.; max.) | 0.67 (-0.84 ; +2.48) | 0.45 (-2.44 ; +2.97) | 0.50 (-1.78 ; +2.52) | -0.31 (-3.40 ; +1.28) | -0.03 (-2.90 ; +2.86) | -0.47 (-2.30 ; +2.44) |
| Standard Deviation | 0.99 | 1.37 | 0.81 | 1.03 | 1.23 | 1.27 |

For the intra-fraction variability we measured 0.02mm (SD 0.24) and an average rotation of 0.05 (SD 0.27) degrees.

Conclusion: Improvement of inter-fraction patient positioning is desirable as this would enable us to use minimal margins. To achieve this, the use of a vacuum bite block would be an option. Since intra-fraction patient position accuracy is high, another possibility would be to use the Robotic table top for on-line positioning correction of both translations and rotations at the start of each fraction.

Future plans: Expanding the tumorsites treated on the Novalis treatment machine, i.e. prostate tumours, where a decrease in CTV-PTV margin might result in a decrease in toxicity. Here the Exactrac system can be used in combination with implanted markers for on-line position correction.

213

A simple method to correctly account for rotational errors in radiotherapy

M. van Herk M, J. Sonke, P. Remeijer, A. Betgen, J. Lebesque
Netherlands Cancer Institute, Radiotherapy Department, Amsterdam, The Netherlands

Purpose: Several methods exist to measure rotational errors during external beam radiotherapy. Correction of rotational errors, however, is rarely performed.

Tilt and roll couches are being developed for this purpose but these are limited to 2 to 3 degrees rotation due to mechanical limitations and for patient comfort.

Correcting the measured translations while ignoring rotations will lead to an inaccurate alignment for points far away from the isocenter. As long as this point is close the center of gravity of the target the associated errors are small.

In many clinical situations (e.g., head and neck) targets are elongated and asymmetric fields are used to enable field matching.

In these circumstances, it is unsafe to ignore rotations. The

purpose of this study is therefore to develop a framework for correction of rotational deviations in a cone-beam CT guided system.

Method: In order to incorporate rotations in a correction strategy, the user first identifies a point or region of interest that should be aligned with priority. After image registration (including rotations) between the planning CT and the on-line scan (on bone or target), the user converts the registration results into a correction that optimally aligns the region of interest given the degrees of freedom available to the correction mechanism.

In the first implementation, the region of interest is a point centered in the GTV and the correction is just a couch shift. For 24 lung cancer patients and 8 head and neck patients, setup errors of bony anatomy were determined from cone beam CT data including rotations. Next, the proposed correction mechanism was applied and differences in translation were determined.

Results: The SD of rotations was around 1.0 degrees (random and systematic) for the head and neck cases and around 1.3 degrees for the lung cases. The method adjusted the translation by about 1 mm (1 SD) for both tumor sites. For individual cases, however, differences in setup correction of up to 5 mm (head and neck) and 7 mm (lymph nodes) were observed.

Conclusion: We developed a simple method to optimize a setup error correction in the presence of rotational errors using couch shifts only. In essence the method geometrically optimizes the alignment for the target given all degrees of freedom available to the correction strategy. In the future the method will be extended to allow for more degrees of freedom, such as couch rotations.

214

How important is the time from positioning to treatment beam off in IGRT for prostate cancer?

M. Bjork, H. Nystrom

The Finsen Center, Copenhagen University Hospital, Copenhagen, Denmark

Image Guided radiotherapy (IGRT) of prostate cancer guided with implanted markers and online an image system has made the delivery of highly conformal dose distributions with tighter margins possible. However, if combined with IMRT a considerable prolongation of the beam delivery time has to be taken into account in the design of margins. It may also require more frequent verification of the actual prostate position and re-positioning of the patient during the treatment fraction to facilitate margin reduction. The aim of this study was to identify and quantify time trends in the prostate movements over the course of a fraction and evaluate the consequences for the margin size.

Materials and Methods: A newly installed image guided system (ExacTrac x-ray 6D) was used to survey intra fraction prostate movements by means of three implanted gold markers. The system utilizes two fully integrated positioning systems; IR camera imaging and kV x-ray imaging, with an origin coincident with the treatment machine iso center.

The patients were treated with 5 to 7 coplanar IMRT fields using dynamic MLC (BrainLAB m³) and sliding window technique (BrainLAB/Varian Novalis). With this delivery technique the time span from patient positioning to the completion of a fraction typically varies from 10 to 20 minutes.

The initial patient set up was guided by the IR camera system and external body markers attached to the patient surface. Repositioning of the patient according to the prostate localisation was accomplished using the automatic marker detection in the kV x-ray imaging system. The coordinates for the prostate markers along with the precise time were recorded before and just after each treatment. Prostate coordinates (x, y and Z) were correlated with the time between the images ranging from 2 to 20 minutes and the displacement in 3D was calculated as a function of time.

Results: Preliminary results evaluated from a limited group of patients, indicate that a time trend exists in the intra fraction prostate movements. Results from the first 10 patients will be presented and the importance of time referring to the design of margins discussed.

We will present results from the first 10 patients and the importance of time referring to the design of margins will be discussed.

215

Changes in patient setup and bladder volume during irradiation of bladder cancer patients

A. Betgen, M. Van Herk, H. Lotz, F. Pos, P. Remeijer, J.

Sonke

Netherlands Cancer Institute, Radiotherapy, Amsterdam, The Netherlands

Introduction: Setup errors and especially organ motion are two important issues in high precision radiotherapy for bladder cancer. We are developing a protocol for image-guided radiotherapy of bladder cancer, based on a cone-beam CT-scan (CBCT), which is integrated with one of our linear accelerators. Currently we are using bony anatomy registration alone, but in the near future we also want to use soft tissue registration in combination with an on-line correction protocol. However, due to a short time interval between registration and actual treatment, important issues with this approach are intra-fraction motion and bladder filling. The purpose of this study is to assess those errors.

| | Intra-fraction motion (mm) | | | Inter-fraction motion (mm) | | |
|----------|----------------------------|------|------|----------------------------|------|-----|
| | L-R | C-C | A-P | L-R | C-C | A-P |
| Mean | 0.0 | -0.2 | -0.6 | 0.4 | -0.7 | 0.4 |
| σ | 1.0 | 0.6 | 0.6 | 2.5 | 1.4 | 2.2 |
| Σ | 0.4 | 0.5 | 0.5 | 1.0 | 1.0 | 1.1 |

Materials & Methods: Intra-fraction motion was measured in 9 patients (55 scans), by acquiring a CBCT just before and directly after irradiation. Patients were instructed to empty their bladder and drink 250cc water, one hour before irradiation. Time interval between the scans was 10 minutes on average (range 9–12min). Both scans were matched to the reference planning CT-scan using bony anatomy registration. The difference between the registrations was defined as the intra-fraction motion, i.e., its mean corresponds with a time trend. The variation was analyzed in terms of random and systematic components to assess their contribution to the margin size. To investigate bladder volume changes, the bladder was delineated on all scans and the difference in volume was determined.

Results: The intra-fraction motion was very small compared to the inter-fraction setup errors.

We measured an increase of bladder volume for all patients. Most changes in the shape of the bladder were found at the cranial-ventral part of the bladder (5.5 mm on average). The inter-fraction variation in bladder filling was small, with a mean SD of 0.5 cc/min. However, we found a large variation in inflow rate between the individual patients (1.2 to 9.6 cc/min), despite the drinking protocol.

Conclusions: Intra-fraction motion is negligible compared to other treatment errors. The inflow rate for the individual patient is reproducible and therefore we can predict the increase of volume during irradiation. This is especially important for cranial-ventral located bladder tumors, as an increase of volume can result in a shift of the position of the tumor.

216

Intra-fraction motion of immobilized brain and head & neck patients

M. Hoogeman, H. Marijnissen, P. Levendag, B. Heijmen

Erasmus MC Daniel den Hoed Oncology Center, Rotterdam, The Netherlands

Purpose: to quantify intra-fraction motion of immobilized brain and head & neck patients. These data may be used to decide on the required margins in online set-up correction protocols in relation with the imaging frequency during a fraction.

Methods: We analysed the intra-fraction motion of 8 patients, who were immobilized with a thermoplastic mask. The motion was recorded by the image-guidance system of the robotic CyberKnife treatment unit. This system consists of two kV X-ray tubes attached to the ceiling of the

treatment room and two imaging flat panels mounted on the floor. During each treatment fraction on average 35 orthogonal image pairs were acquired over a time period of on average 48 minutes. The images were registered to DRRs; the skull of the patient was used to obtain the translations and rotations. We analysed the intra-fraction motion by grouping the translations and rotations according to the time difference between two localizations. The time differences were discretized to 30 s and the collected translations and rotations within this time interval were averaged. By this method we obtained the mean displacement as a function of the time between two localizations for every patient and fraction. Next, we calculated amongst others the group-mean displacement together with the standard deviation (SD), and the maximum displacement as a function of time.

Results: Over a period of 40 min the group-mean translation was below 0.3 mm and the group-mean rotation below 0.2 degrees for all components. The SD increased over time: from 0.2 mm (quadratic sum over all directions) at a 30-s time interval, to 0.3, 0.7, and 1.0 mm at a time interval of 5, 20, and 40 min respectively. For the three rotations we observed the same trend: the SD increased nearly linearly to 0.5° over a time period of 30 min. The maximum translation was found in the SI direction and saturated at 3.0 mm after 50 min. The maximum rotation of 2.8° was found around the AP axis after 28 min.

Conclusions: The data showed no overall time trend in the patient position for the whole patient group, although the SD indicated a with time increasing displacement for the individual patients. For conventional treatment times (<15 min) the modest intra-fraction motion could be accommodated by a margin around the CTV. For longer treatment times we prefer to repeatedly update the patient position with a time interval of <5 min and correct for displacements as is performed by the CyberKnife system.

Wednesday, September 28, 2005
Proffered Papers

IMRT II

217

Development of a scanning system for intensity modulated radiation therapy with photon pencil beams

B. Andreassen¹, R. Svensson¹, H. Danared², A. Brahme¹

¹Karolinska Institute, Medical Radiation Physics, Stockholm, Sweden

²Stockholm University, Manne Siegbahn Laboratory, Stockholm, Sweden

The increasing cancer incidence requires more accurate and cost-effective diagnostic as well as therapeutic methods. Intensity modulated radiation therapy is now rapidly being introduced at many radiation therapy departments with a clear trend towards radiobiological treatment planning using 4D-diagnostic imaging and -treatment delivery. Therefore a magnetic system for scanning of narrow photon pencil beams has been developed for fast 4D-IMRT. The magnetic scanning system has been modelled in full 3D taken into account all aspects such as fringing field, magnetic leakage and cooling. The magnetic system consists of two perpendicular scanning magnets, a bending magnet and a purging magnet placed after a thin bremsstrahlung target and in the same plane as the last scan magnet. The scanning magnets operate in orthogonal planes and the first scanning magnet (bending plane) is placed so that the image of its scanning centre lies near the effective centre of the second scan magnet (cross plane). In this way a very compact deflection system is obtained, with the position of the effective radiation source coinciding for the two orthogonal planes. The focus of the intrinsic electron beam is at the top of the target placed near the end of the last scanning magnet. The composition and thickness of this target determines the energy of the transmitted electrons and the full width half maximum (FWHM) of the photon beam. Here the target is made of 3 mm beryllium creating a therapeutic beam of 10-15 mm (FWHM) for an incident electron beam of 70-50 MeV. The transmitted electron beam has only lost around 0.5-1.0 MeV in the target and must be removed from the therapeutic beam. Therefore downstream of the target a strong and fast purging magnet integrated with an electron collector has been developed. The purging magnet operates in the same plane as the last scanning magnet and deflects the transmitted high energy electrons to the same area on the electron collector independent of the direction of the scanned photon beam. The overall design of the treatment head is compact and the narrow photon beam will allow a very accurate dose delivery particularly when combined with a thin efficient leaf collimator designed for pencil beam IMRT.

218

Dose Volume Benefits and Delivery Accuracy of a Novel Rotating Collimator Precision IMRT Technique

K. Otto¹, M. Schmuland²

¹British Columbia Cancer Agency – Vancouver, Medical Physics, Vancouver, Canada

²University of British Columbia - British Columbia Cancer Agency, Physics, Vancouver, Canada

The purpose of this work is to evaluate a new IMRT planning and delivery method that fully exploits MLC rotation. The feasibility of using full MLC rotation in IMRT leaf sequencing was previously investigated where it was shown that there are advantages in: (1) improved spatial resolution of fluence maps, (2) increased flexibility in generating aperture shapes and (3) decreased systematic error due to interleaf effects. These studies were limited to single fields and therefore did not quantify the level of improvement for multi-field 3-dimensional IMRT dose distributions. In this study we evaluate the ability of the rotating MLC (RMLC) IMRT technique to generate conformal 3D dose distributions. Also, we summarize the results of a series of measurements used to evaluate the dosimetric accuracy of this technique.

The delivery process for RMLC IMRT is similar to conventional step-and-shoot techniques except that the collimator is also rotated with each MLC 'step'. For each segment the collimator rotates to the desired angle, the MLC leaves move to the desired positions and the beam is activated for a specified number of MU. The process repeats until all segments have been delivered.

IMRT plans for a geometric phantom, a prostate and a nasopharynx recurrence were generated. Dose distributions were measured using a water equivalent multi-plane film dosimetry phantom (MDX Medical Inc). DVH analysis and 3D dose comparisons show that target coverage is equivalent or better with collimator rotation. Healthy tissue sparing is improved with collimator rotation, more so for the smaller, more complex, nasopharynx target. It is also shown that improvements in radiation efficiency (decreasing MU) with RMLC will increase healthy tissue sparing. There is a 33.7% and 23.3% reduction in monitor units for the prostate and nasopharynx plans respectively. Finally, gamma factor and dose difference analysis of measured dose distributions indicate that RMLC dose distributions can be delivered accurately and reproducibly on a Varian cI21ex linac, confirming that the RMLC technique is ready for clinical implementation.

219

A comparison of two probabilistic methods for intra-fractional re-optimization in IMRT

R. Flynn¹, J. Unkelbach², U. Oelfke², R. Jeraj¹, T. Mackie¹

¹University of Wisconsin, Medical Physics, Madison, WI, USA

²Deutsches Krebsforschungszentrum, Medical Physics in Radiation Therapy, Heidelberg, Germany

Purpose: Real-time imaging methods can provide anatomical information which can in principle be used for intra-fractional re-optimization of the radiation delivery. We investigate two strategies that utilize real-time imaging information for intra-fractional re-optimization in a rotation therapy case.

Methods: A multiple-rotation tomotherapy treatment is simulated for a radially symmetric case in a homogeneous cylindrical phantom. Knowledge of tumor location is represented in terms of Gaussian probability density functions (pdfs) with widths that are decreasing from one rotation to the next. Widths were assumed to inversely decrease with the number of rotations. The pdfs are updated on-the-fly throughout treatment and are used to calculate the expectation value and the variance of the dose delivered at each point in the phantom over the remaining treatment period. During each rotation a re-optimization for the remaining rotations is performed using the most recently available information and the dose residual. Two quadratic objective functions are examined for the re-optimization step. The first objective function simultaneously minimizes the quadratic difference between the expected and prescribed dose plus the variance of the dose. The second objective function is a heuristic simplification that neglects the variance term.

Results: Inclusion of the variance term resulted in much more conservative dose distributions for early rotations. An extremely low dose was delivered in the first two of four rotations and nearly all of the dose was delivered in the last rotation. Optimization without the variance term resulted in a less conservative dose delivery in the early rotations, but very sharply peaked fluence profiles for later rotations. The dose variances during early rotations were substantially higher after the removal of the variance term from the objective function.

Conclusion: Inclusion of the dose variance term in the optimization results in fluence profiles that are not sharply peaked and hence safely deliver the dose to the tumor in later rotations. Removal of the variance term from the objective function leads to a gradual dose delivery over early rotations with a very sharply peaked fluence profile for the last rotation. Hot spots may occur after the actual treatment

since the expectation value of the dose is not realized for the individual patient, which makes the benefit of this strategy questionable.

220

From a priori to a posteriori decision-making in the design and selection of an optimal IMRT treatment plan

A. Hoffmann, H. Kaanders, H. Huizenga

Radboud University Nijmegen Medical Centre, Department of Radiation Oncology, Nijmegen, The Netherlands

Introduction: Different methods and procedures for radiobiological treatment plan evaluation and optimization have been presented in the past. Typically, a single score function balancing tumour control probability (TCP) versus normal tissue complication probability (NTCP) using weights to express their relative importance is used to guide the optimization process. Unfortunately, this score function requires the articulation of a (physician-dependent) *a priori* trade-off between benefit and risk without knowing the sensitivity of the optimization result to changes in the weights. A dose-level scaling optimization strategy has been suggested as an alternative to find an optimal treatment plan according to a *posteriori* articulated risk-balancing preferences. Here, we suggest an optimization approach for which no *a priori* predilection of TCP and NTCP is required, and show how changes in TCP and NTCP interrelate. A comparison with the dose-level scaling approach is presented.

Methods: For a bi-objective inverse treatment planning optimization problem having only one TCP and one NTCP objective, first the Therapeutic Operating Characteristic (TOC) representation for evaluation of the of dose-level scaling approach is presented. Then, a multi-objective optimization approach (cf., Küfer et al. 2000) is used to find Pareto-optimal solutions by maximizing TCP under varying NTCP constraints. These solutions have the characteristic that improving TCP cannot be accomplished without deteriorating NTCP and vice versa. In the TCP-NTCP space, the set of Pareto-optimal plans is represented by the Pareto frontier (PF) that displays the spectrum of optimal treatment plans for different risk-taking preferences. The relative position and shape of the TOC and PF are compared.

Results and Discussion: The TOC depicts how TCP and NTCP are interrelated as an effect of dose-level scaling. It represents the trajectory of dose-level scaling as a parametric plot of benefit versus injury with the absorbed dose as a parameter. We demonstrate how the TOC can be used to estimate the optimum dose level by maximizing a single objective function incorporating an *a priori* articulated trade-off between TCP and NTCP. For generation of the PF, no *a priori* predilection of TCP and NTCP is required. Instead, multiple optimizations have to be performed. The PF defines a unique upper bound on the set of TOC's from which the physician and physicist can select an optimal plan that is tuned to their preferences.

Küfer KH, Hamacher HW, Bortfeld T. A multicriteria optimization approach for inverse radiotherapy planning. Proceedings of ICCR 2000. pp. 26-28.

221

Optimization using multicriteria decision making for individualization of complex treatment protocols

R. Ten Haken, K. Jee, K. Vineberg, D. McShan, E. Ben-Josef, C. Pan

University of Michigan, Radiation Oncology, Ann Arbor, MI, USA

Introduction: Many modern protocols specify multiple treatment goals for several tumor and/or normal tissue subvolumes, often in terms of non-dosimetric evaluation criteria. PI an optimization under these circumstances often requires compromise among general population-based protocol criteria. A flexible optimization scheme capable of characterizing patient-specific tradeoffs among conflicting goals is examined in this context.

Methods: A typical complex protocol for liver tumors includes the multiple goals of maximizing the EUD of the primary PTV, maintaining a minimum EUD to a sub-clinical PTV, while simultaneously sterilizing predetermined subportions of these volumes that could potentially make the patient surgically operable; all while also maintaining a normal liver iso-NTCP level (potentially incorporating the resection portion of the liver) and also respecting dose/volume constraints to stomach, duodenum, kidneys and cord. This and other similarly complex protocols for pancreas and lung tumors were studied in 24 patients.

IMRT optimization used a multicriteria objective prioritization strategy based on preemptive goal programming. The methodology allowed 1) definition of multiple optimization goals for each structure, 2) categorization based on their priorities and 3) addressing them in a staged order. In practice, prior stage results were constrained for subsequent stages, gradually reducing the feasible solution space. This hierarchical optimization process also produced local sensitivity information (based on Lagrangian multipliers) that quantified correlations among the preceding constraints and the existing objectives; information that identified which planning goals were responsible for underachievement of current stage objectives. Based on this information, patient-specific selective relaxation of planning goals was investigated.

Summary: For difficult liver, pancreas and lung tumor protocol patients, examination of the correlations between target and normal structure objectives indicated small patient-specific relaxations of dose/volume constraints to external OARs which lead to 2-8 Gy increases in EUD over the already substantial EUDs to the targets obtained in the initial optimization.

Conclusions: Multicriteria decision making, with its staged examination of correlations between constraints and plan objectives, permits clinically relevant individualization of IMRT treatment plans for complex treatment protocols. Supported by NIH P01-CA59827

222

Elastic motion compensation via a dynamic MLC (dMLC) technique

S. Webb

The Royal Marsden NHS Trust, Joint Department of Physics Sutton, Surrey, UK

Purpose: A major remaining problem in delivering radiotherapy, specifically intensity-modulated radiation therapy (IMRT) is the need to accommodate and correct for intrafraction organ motion. The developing availability of 4D computed tomographic images forms the basis of the new field of image-guided IMRT. It is important to understand the effects on delivered dose of organ motion during IMRT and to suggest a practical correction strategy.

Method: The "stretch-and-shift-the-planned-modulations" strategy is proposed and a practical method to deliver this is explained. This practical strategy is based on a modification of the dynamic multileaf collimator (dMLC) IMRT method whereby the leaves are arranged to track in tandem the organ motion of the patient. E.g if organs move due to patient breathing the leaves "breathe" in tandem.

Results: (i) A geometric construction has been developed to predict the patient-frame motion-affected intensity-modulated beam (IMB) from the intersection of the body position trajectories with the leaf trajectories appropriate to an "intended" (in the absence of motion) IMB. (ii) When the leaf trajectories do not "breathe" but the body positions do, the degraded IMB can be computed by integrating this construction over all possible phases. The result is identical to the dwell-time-weighted mean of the intended modulation over the motion. This proves that the dMLC technique acts exactly like a compensator even in the presence of organ motion. (iii) When the leaf trajectories "breathe" and the body locations identically breathe the reconstructed IMB is identical to the intended IMB ("phase locking"). (iv) When the leaf trajectories breathe (with a single starting phase) and the body locations breathe the reconstructed IMB, averaged over all phases, is quite different to the intended IMB even though

all other parameters are correctly matched. (v) When the leaf trajectories breath (with a single starting phase) and the body locations breath the reconstructed IMB averaged over a small range of phases is not too different from the intended IMB. (vi) When the leaf trajectories breath (with a single starting phase) and the body locations breath the reconstructed IMB, averaged over a small range of phases, is very different from the intended IMB when any or all of the other motion parameters: period, shape and amplitude are mismatched.

Conclusion: "Phase-locked leaf tracking" can overcome the effects of regular rhythmic motion. Any other mismatched leaf motion is incorrect.

223

Implementation of Monte Carlo calculated beamlet dose distributions in a direct aperture optimization algorithm for IMRT

A. Bergman¹, K. Bush², M. Milette¹, I. Popescu¹, K. Otto¹, C. Duzenli¹

¹British Columbia Cancer Agency, Medical Physics, Vancouver, Canada

²British Columbia Cancer Agency, Medical Physics, Victoria, Canada

In this work we introduce a Monte Carlo (MC) calculated beamlet dose distribution matrix into a direct aperture optimization (DAO) algorithm for IMRT planning. The goal is to assess if accurate tissue inhomogeneity information input into the DAO inverse planning algorithm will improve the accuracy and efficiency of the optimized treatment plan. Several authors have shown that the presence of small fields and/or inhomogeneous materials in IMRT treatment fields can cause significant dose calculation errors for algorithms that are unable to accurately model electronic disequilibrium. This issue may also affect the IMRT optimization process because the dose calculation algorithm may not properly model difficult geometries such as targets close to low-density regions (lung, air etc.). A clinical linear accelerator head is simulated by Monte Carlo (using BEAMnrc, NRC, Canada). A phase space plane is recorded below the collimating jaws. Novel, locally built software subdivides the resulting phase space into 2.5 x 2.5 mm (at 100 cm) beamlets. Each beamlet is projected onto a patient-specific phantom (2.5 x 2.5 x 2.5 mm³ voxels) at the relevant gantry angle. The beamlet dose contribution to each phantom voxel in an organ of interest is established. This information is input to an in-house inverse planning system derived from DAO techniques described by Shepard et al.. DAO directly modifies the shape/weight of multi-leaf collimator (MLC)-defined apertures. The MLC aperture optimization includes MLC dosimetric properties such as transmission and physical limits of motion. The deliverable leaf sequence optimized with the MC dose input and the conventional pencil beam kernel (PBK) dose input are compared. Improvement in efficiency is assessed by comparing the MC DAO approach with traditional fluence-based optimization for a clinical head and neck case. A forward calculation with MC is used to compare final dose distributions. MC simulation can generate accurate beamlet dose distributions in traditionally difficult-to-calculate regions. Combining the DAO approach with the MC beamlets results in significant improvement in both optimization efficiency and accuracy of the final dose calculation, particularly in regions of tissue inhomogeneity.

224

Dosimetric implications of intentional skin dose with IMRT

S. Gulliford¹, H. James¹, C. MacKenzie², J. Le Vay³, E.

Sherwin³, S. Smith¹, R. Perry², A. Poynter¹

¹Suffolk Oncology Centre, Medical Physics, Ipswich, UK

²Suffolk Oncology Centre, Radiotherapy, Ipswich, UK

³Suffolk Oncology Centre, Clinical Oncology, Ipswich, UK

Aim: To plan, deliver and verify a therapeutic skin dose for a patient with extensive metastatic skin disease progressing

from primary breast cancer using IMRT.

Method: A patient presented with rapidly progressing skin involvement extending across much of her upper torso. Previous treatment included radiotherapy with radical intent, chemotherapy and mastectomy with skin flap. Further chemotherapy failed to control the spread of disease. Treatment intention was to deliver a uniform dose across a large area whilst taking into account sensitive underlying structures. The extent of the disease required matching of a number of electron fields so an IMRT approach was considered as an alternative. The patient was fitted with 1cm of bolus and thermoplastic shell and a CT scan was obtained in the treatment position. The scan was transferred to the treatment planning system (TPS) where the external body contour incorporated the bolus. A geometry-based optimisation PTV was defined extending 0.5cm into bolus and encompassing bi-lateral skin disease. Lung, heart, liver and spinal cord OAR volumes were also created. 7 equi-spaced treatment fields were applied and dose constraints for PTV and OARs defined. The plan was optimised to produce a homogenous dose to the defined skin area with a prescription of 50Gy in 25 fractions. Plan verification consisted of standard pre-treatment dose and fluence phantom measurements, routine portal imaging and in-vivo dosimetry using TLDs positioned on the skin surface beneath the bolus.

Results: Pre-treatment verification agreed with the TPS calculation to within 1% to a defined point within the PTV with agreement over the fluence map of 4% for all 7 fields. Patient setup reproducibility was within protocol over the course of treatment and in-vivo dosimetry showed an average difference from the predicted TPS values of -1.8%. Gamma analysis showed that small uncertainties in positioning of the TLDs accounted for some of the discrepancies seen.

Conclusion: This extreme patient presentation challenged current experience of IMRT as a process for treating localised, deep-seated radical disease. The dosimetric analysis for this case was in good agreement with expected calculated doses underlining the successful translation to palliation of widespread superficial disease with IMRT.

225

IMRT dose distributions for ethmoid sinus cancer calculated by five different treatment planning systems

L. Paelinck¹, B. De Smedt², N. Reynaert², M. Coghe¹, W. De

Gersem¹, C. De Wagter¹, B. Vanderstraeten², H. Thierens²,

W. De Neve¹

¹University Hospital Ghent, Radiotherapy, Ghent, Belgium

²University Ghent, Medical Physics, Ghent, Belgium

Purpose: Intensity-modulated treatment plans of patients with ethmoid sinus cancer treated at an Elekta were calculated by five different dose calculation algorithms and the dose-volume histograms (DVHs) of the planning target volume (PTV) and the optical chiasm were compared.

Materials and methods: Ten step-and-shoot intensity-modulated treatment plans were enrolled in this study. The presence of large air cavities and small critical structures constitutes a real challenge for dose calculation algorithms. Each intensity-modulated treatment plan is created and optimized with GRATIS and home-made software and is subsequently recalculated by two superposition convolution algorithms (Helax-TMS and Pinnacle) and two Monte Carlo algorithms (Peregrine and MCDE*). The DVHs for each patient and each dose calculation algorithm were assessed. The mean DVH of each dose calculation algorithm over the ten patients was obtained by calculating the mean dose at every 0.5 % volume level. Statistical analysis was performed by one way ANOVA for repeated measurements and multiple pairwise comparisons was done by the method of Tukey. A p-value less than 0.05 was considered statistically significant.

Results: In the shoulders of the mean DVHs of the PTV, no statistical differences were found between the five different treatment planning systems (figure). In the tails of the mean DVHs of the PTV, significant differences were found between

all dose calculation algorithms, except between Helax-TMS and Pinnacle and between Pinnacle and Peregrine. The tails of the mean DVH of the PTV are very large for the Monte Carlo code MCDE. An explanation for this was found in the presence of large air cavities contained in the PTV. In these air cavities, relatively few particles will interact in comparison with the situation in the surrounding tissues and this give rise to more statistical noise. Significant differences were also found for the mean DVHs of the optical chiasm. The deviation of the Peregrine DVH is understood and reported**.

Conclusions: All dose calculation algorithms investigated result in different DVHs. The differences between the dose distributions themselves are presumably even greater.

* Reynaert N, De Smedt B, Coghe M *et al* MCDE: a new Monte Carlo dose engine for IMRT *Phys Med Biol* 2004 **49** N235-241

Reynaert N, Coghe M, De Smedt B *et al* The importance of accurate linear accelerator head modeling for IMRT Monte Carlo calculations *Phys Med Biol* 2005 **50 831-46

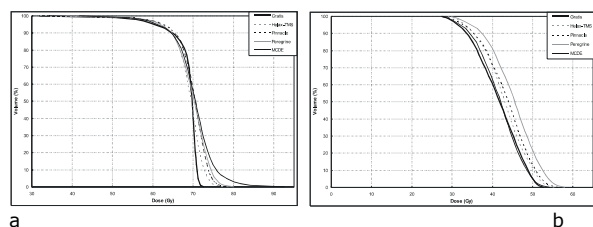


Figure: Mean DVH of a) PTV and b) optic chiasm for the five dose calculation algorithms.

Novel technologies

226

Design of the MRI accelerator

*B. Raaijmakers*¹, *U. Van der Heide*¹, *A. Raaijmakers*¹, *J. Overweg*², *K. Brown*³, *J. Welleweerd*¹, *C. Bakker*⁴, *J. Lagendijk*¹

¹University Medical Center Utrecht, Radiotherapy, Utrecht, The Netherlands

²Philips Philips Research Hamburg, Hamburg, Germany

³Elekta, Crawley, UK

⁴University Medical Center Utrecht, Radiology, Utrecht, The Netherlands

The UMC Utrecht, together with Elekta and Philips Medical Systems, is pursuing a precise, soft-tissue based, on-line position verification and treatment monitoring system for image guided radiotherapy (IGRT). Basically the design is a modified 1.5 T Philips Achieva MRI scanner with a small, single energy (6 MV) accelerator rotating around it.

To magnetically decouple both systems, active magnetic shielding is applied to minimise the magnetic field at the components of the accelerator and completely nullifying the magnetic field at the location of the accelerator gun section. To allow beam transmission through the midplane of the closed bore MRI system, the beam pathways are being homogenised and minimised.

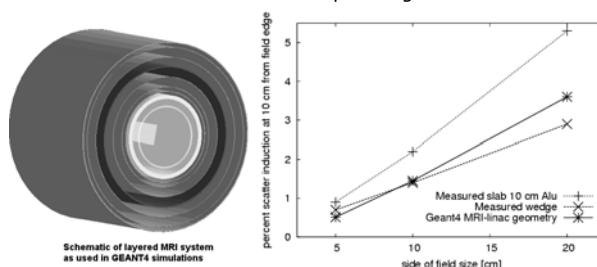
The treatment characteristics, both MR imaging and irradiation, have been investigated in a technical feasibility study. The radiation beam characteristics have been studied using Geant4 monte carlo simulations and in an experimental setting. The dose deposition in the presence of a transverse magnetic field is affected, an increased penumbra and a different dose build-up around air cavities were found. Also the scatter induction by transmission through the modified MRI system was studied. As an example, the figure shows the scatter induction as function of the field size compared with that by an internal wedge.

With respect to the MR imaging a special gradient coil set has been designed with a radiation window allowing a 24 cm field

size in the caudal cranial direction for every gantry angle. The gradient linearity within a spherical volume of approximately 25 cm diameter is similar to an unmodified gradient coil. The main magnet, after the required modifications for active shielding and minimising the radiation thickness, achieves comparable field homogeneity as an unmodified magnet. The results from this design study have been translated into manufacturing specifications for a prototype magnet.

The accelerator components must be compact in order to be mounted and rotate in a ring around the MRI. Since the magnetic field is minimised at this location, commercially available components can be used.

We have concluded that integrating a radiotherapy accelerator and MRI functionality is technically feasible and are now quantifying the treatment characteristics of a prototype in detail. Ultimately the system may be used for daily treatment optimisation by providing imaging information for on-line treatment planning.



227

Dose distribution in a patient anatomy for an integrated MRI-linear accelerator system: boosting the dose around air cavities using the magnetic field

A. Raaijmakers, *B. Raaymakers*, *J. Lagendijk*
UMC Utrecht, Radiotherapy, Utrecht, The Netherlands

The UMC Utrecht, in a collaboration with Elekta and Philips Medical Systems, is developing a new IGRT system, integrating a MRI-scanner with a linear accelerator. The project aims for on-line, soft-tissue based position verification and treatment monitoring. In the design of the apparatus, the 6MV photon beam will penetrate the MRI-scanner from outside and dose deposition will occur in the presence of a homogeneous 1.5 T caudal cranial magnetic field. Therefore, the dose distribution will be affected by the Lorentz force. This influence was investigated using GEANT4 Monte Carlo simulations.

First, convoluted photon pencil beams were used to investigate the dose deposition in homogeneous [1] and inhomogeneous phantoms [2]. The latter showed a dose increase of 40% at tissue-air boundaries, because electrons leaving the phantom are forced back into the phantom by the Lorentz force. This phenomenon will be referred to as the electron return effect (ERE). The ERE causes a very localized dose deposition at the tissue-air interface, whereas conventionally an underdosage around air cavities occurs due to fact that the electrons in air scatter out of the field. The ERE has the potential to compensate for this underdosage and this work is the first attempt to study the ERE around air-cavities in a real patient anatomy.

A voxelised patient anatomy can be imported into GEANT4. Using a unidirectional photon beam with a 6MV energy spectrum, the ERE can clearly be shown around the oropharynx, see figure 1. In the presence of a magnetic field the dose at the proximal side of the air cavity is increased and at the distal side decreased compared to the situation without magnetic field. Opposing beams compensate for the overdosage [2]. Whether opposing beams in a realistic anatomy can be used for full compensation is being investigated.

The dose distribution in real patient geometries can be simulated by importing voxelised MRI or CT-data in GEANT4. Simulations with a magnetic field clearly show the effects that were found earlier in phantom geometries and indicate

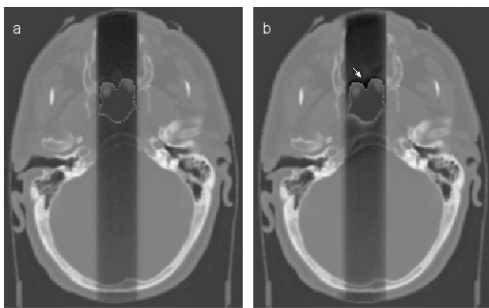


Figure 1. Qualitative image of ERE around the oropharynx. Dose distribution is overlaid on CT-image for $B=0$ (a) and $B=1.5\text{ T}$ (b). Arrow indicates ERE.

promising possibilities to exploit the ERE to prevent underdosage near air cavities.

1. Raaijmakers et al. "Integrating a MRI scanner with a 6 MV radiotherapy accelerator: dose deposition in a transverse magnetic...", PMB 49 p. 4109-4118
2. Raaijmakers et al. "Integrating a MRI scanner with a 6 MV radiotherapy accelerator: Dose increase at tissue-air interfaces in a lateral magnetic field due to...", PMB 50 p. 1363-1376

228

Potential efficacy of a couch with restricted out-of-plane rotations for on-line corrections.

Y. van Herten, J. van de Kamer, N. van Wieringen, J. Wiersma, A. Bel

Academic Medical Center, Radiotherapy, Amsterdam, The Netherlands

Purpose: To investigate the effect of on-line correction of rotations using a table-top with 3D rotation option¹.

Methods: We acquired CT datasets of patients with prostate cancer, for which conformal 4-field boxtechnique plans (10 MV) without any PTV margin were made. The 95% iso-dose encompassed the CTV exactly. The seminal vesicles were not included in the CTV.

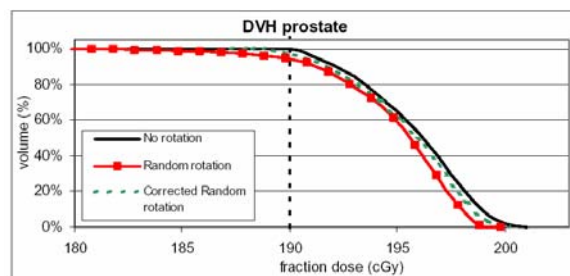
The average systematic error for all patients was set to 0° for rotations in all directions; the SD in this error was 5.1°, 2.2° and 1.3° around the LR, CC and AP axes. Since all translation errors were set to zero, the centre of rotation is the iso-centre of the plan. With these parameters 5 different patientspecific systematic rotation errors were randomly determined assuming the appropriate Gaussian distribution.

For these situations 35 fractions (2Gy/fraction) were simulated with SD 3.6° (LR), 2.0° (CC) and 1.6° (AP). This provided a simulated 3D dose distribution for 5 cases, including both systematic and random deviations.

These simulations were repeated with restricted rotation corrections for each treatment. For patient safety this limit was set to 3° in all directions, implying that if an on-line correction protocol is used errors < 3° can be reduced to 0° but an error of e.g. 5.4° can be reduced to 2.4°. This provided a 3D dose distribution accounting for errors and the restricted possibilities to reduce them. For all these situations DVHs were constructed and evaluated.

Results: The figure shows DVH curves for the original plan, for one of the 5 plans with systematic and random rotations and the corresponding plan with maximally corrected rotations.

For the non-corrected plans the 95% iso-dose covered on average 95% of the CTV, for the corrected plans this increased to 98%.



Discussion: The effect of rotations proves to be modest for the sphere-like prostate. However, if seminal vesicles are included in the CTV the effect of rotations is probably larger. The presented method will be used to study this. Additionally this method will be used for other tumour sites. In general, the presented procedure can be used to determine PTV margins based on realistic systematic and random errors and realistic patient geometries.

Conclusion: Using an on-line position verification protocol in which all rotations can be corrected by 3° can improve the dose distribution.

¹ e.g. HexaPOD table (Medical Intelligence)

229

Optically stimulated luminescence (OSL) of carbon-doped aluminum oxide (Al₂O₃:C) for film dosimetry in radiotherapy

V. Schembri¹, J. Gray², C. Ochampaugh², B. Heijmen¹

¹Erasmus MC / Daniel den Hoed Cancer Center, Radiation Oncology, Rotterdam (The Netherlands)

²Landauer inc., Glenwood (Illinois), USA

Introduction and Purpose: Conventional X-ray films and radiochromic films have inherent challenges for high precision radiotherapy dosimetry. Therefore, we have initiated studies on film dosimetry based on optically stimulated luminescence (OSL) of carbon-doped aluminum oxide (Al₂O₃:C) for two-dimensional dosimetry. Stimulation of irradiated Al₂O₃:C with green light (~500 nm) from light emitting diodes (LEDs) results in emission of blue luminescence (~420 nm), proportional to the absorbed dose of ionizing radiation. Optically stimulated luminescence materials operate much the same way as TL phosphors except that the recombination luminescence is stimulated optically rather than thermally. Thus, OSL dosimetry avoids problems caused by heating of TLD dosimeters. In addition, for thermally stimulated materials the entire sample must be imaged at one time, while for optically stimulated materials can be scanned out line by line, which is much a less expensive approach. For the megavoltage energy range the mass energy absorption coefficients and mass stopping powers of Al₂O₃:C are very similar to those of water. The purpose of the research is the assessment of the basic characteristics of OSL in Al₂O₃:C for film dosimetry in radiotherapy and the development and evaluation of procedures and equipment for OSL film dosimetry.

Materials and Methods: Single crystals of Al₂O₃:C are ground into a powder and mixed with a polyester base. The mixture is deposited on polystyrene films. The thickness of the films is 0.3 mm. The films can be cut to any size or shape, and are as flexible as conventional x-ray films. Measurements have been performed in 6 MV and 18 MV photon beams, with different field sizes (4x4, 10x10, 20x20 and 30x30 cm²), and depths (dose max, 5, 10, 20 and 35 cm). OSL readings were compared with absolute doses measured with an ionization chamber (NE2571).

Results: For the large range of field sizes and depths, the ratio OSL-reading/ ionization chamber dose was constant within about 2%, both for the 6 MV and the 18 MV beams. The reproducibility was better than 2%.

Conclusions: The preliminary experiments for 6 MV and 18 MV beams show that Al₂O₃:C OSL is a promising material for two-dimensional radiotherapy film dosimetry. Data will be

presented for energies ranging from ^{60}Co to 23 MV, for MLC-shaped fields and for applications in IMRT dosimetry.

230

3D controlled regional hyperthermia equipment to improve tumour temperatures.

H. Crezee¹, P. Kok¹, R. Westendorp², J. Wiersma¹, G. van Stam¹, J. Sijbrands¹, A. Bel¹, P. van Haaren¹

¹Academic Medical Centre, Radiation Oncology, Amsterdam, The Netherlands

²Radiotherapeutisch Instituut Stedendriehoek en Omstreken, Deventer, The Netherlands

Introduction: Hyperthermia is a powerful chemo and radiosensitiser and is successfully applied for cervical tumours and other malignancies. There is a strong dose-effect relation, but achieving the goal tumour temperature of 43°C for 1 hour is often a challenge due to high, treatment limiting temperatures in normal tissue (hot spots). Our present AMC-4 regional hyperthermia system is a ring of four 70 MHz RF antennas. Heating systems with better power control, e.g. by increasing the number of antennas, are expected to improve tumour temperatures. We developed an AMC-8 system consisting of 2 rings of 4 antennas. The position of the central power focus created by the 8 antennas can be directed in 3D towards the tumour by adapting the phase settings.

Purpose: to test the performance of this new AMC-8 system for the E-field distribution, 3D power control and efficiency in comparison with the present AMC-4 system.

Methods: Measurement of the E-field distribution for the AMC-4 and AMC-8 system was performed in a liquid tissue equivalent phantom using an E-field probe.

1) The size and shape of the central power focus were quantified by the radial and axial Full Width Half Maximum (FWHM).

2) 3D control was evaluated by studying the position of the central power focus for different phase settings of the AMC-8 system.

3) Efficiency was determined by measuring the temperature rise in the transversal midplane of a solid tissue equivalent phantom after a short power pulse.

Results:

1) The FWHM of the power focus is larger in the axial and smaller in the radial direction for the AMC-8 system than for the AMC-4 system. This smaller radial FWHM is favourable in preventing hot spots.

2) 3D control: An increase in the phase of the antennas of the second ring of the AMC-8 system results in a well controlled axial shift of the central power focus over 0-10 cm.

3) Efficiency is 90% in the AMC-8 system, versus 60% in the AMC-4 system.

Conclusion: The AMC-8 system has 3D power control, is more efficient and has a more favourable power distribution than the AMC-4 system. This is expected to reduce the incidence of hot spots, and result in a higher tumour temperature. Determination of the clinical benefit of the AMC-8 system is subject of further research.

Supported by the Dutch Cancer Society.



231

Exploring the potentials of helical tomotherapy in head and neck cancers radiotherapy

C. Fiorino¹, I. Dell'Oca², A. Pierelli¹, S. Broggi¹, N. Di Muzio², E. De Martin¹, F. Fazio^{2,3}, R. Calandrino¹

¹Ospedale San Raffaele, Medical Physics, Milano, Italy

²Ospedale San Raffaele, Radiotherapy Department, Milan, Italy

³IBFM CNR, University of Milano Bicocca, Institute H.S. Raffaele, Milano, Italy

Purpose: To explore the potentials of Tomotherapy (TT) in the treatment of head and neck cancers (HNC).

Materials and methods: In a first study (A), Five patients with locally advanced oropharynx or hypopharynx cancer were considered and IMRT Linac (Varian Helios/Eclipse, Linac 600 CD, 6 MV X-Rays) and TT planning were compared in terms of PTV coverage and sparing of parotids (P), mandible (M) and spinal cord (SC). In a second study (B), currently in progress, the goal was to search the limits of TT in sparing other critical structures (mucosae outside PTV with 0.5 cm margin from PTV (MUC), larynx, thyroid, esophagus, sub-mental connective tissue, inner ear) by keeping P, M and SC sparing within acceptable levels. For each patient an initial target (CTV1) including nodal region was contoured and expanded to generate PTV1; then, CTV2 including high risk nodes and CTV3 including only T were defined and the corresponding PTV2/PTV3 were generated (0.5 cm margin). In study A, IMRT and TT plans were optimised to deliver 54 Gy in 30 fractions on PTV1 followed by the delivery of 16.2/15 Gy in 9 fractions to PTV3 and (concomitantly) to PTV2. Dose volume constraints for PTV coverage and OARs sparing (SC, 0.5 cm expanded SC, P, M) were assessed, based on our previous IMRT experience, with the highest priority to SC sparing and PTV coverage. At this moment, study B focused on one nasopharynx patient in both sequential and simultaneous integrated boost (SIB) approaches.

Results: Study A showed a significantly better sparing of P and M with TT with respect to IMRT Linac, especially during the delivery of the first phase (mean dose to P: 20.8 TT vs 26.2 IMRT Linac), a much better coverage of PTVs and greater homogeneity within PTVs with TT.

Study B showed the possibility to deliver SIB while irradiating most of MUC to doses below 20-25 Gy (V30 = 18 %, Dmean = 20.8 Gy) while delivering concomitantly 54 Gy, 61.5 Gy and 64 Gy in 28 fractions to PTV1, PTV2 and PTV3 respectively. Larynx (Dmean = 13.6 Gy), sub-mental connective tissue (Dmean = 24.8 Gy), esophagus (V45 = 9.5 %), thyroid (V45 = 54.5 %) and inner ear (Dmean = 52 Gy) were also efficiently spared. Large gains both in OAR sparing and PTV coverage were evident when comparing these data with a similarly stressed IMRT Linac inverse plan.

Conclusions: Preliminary findings suggest that TT has the potential to significantly improve the therapeutic ratio of HNC. The generation of very rapid dose gradients seems to have the potentials to spare tissues generally difficult to protect with conventional IMRT Linac delivery.

232

Clinical implementation of helical tomotherapy treatments: preliminary experience of dosimetrical measurements of QA patient.

S. Broggi¹, S. Molinelli^{1,2}, G. Cattaneo¹, C. Fiorino¹, N. Di Muzio³, F. Fazio^{3,4}, R. Calandrino¹

¹H.San Raffaele, Medical Physics, Milano, Italy

²Università degli studi di Milano Scuola di Specializzazione in Fisica Sanitaria, Milano, Italy

³H.San Raffaele, Radiotherapy, Milano, Italy

⁴H.San Raffaele IBFM CNR, University of Milano Bicocca Milano, Italy

Aim: to verify and check dosimetrical accuracy between calculated and measured dose distributions for IMRT treatments delivered with a clinical Helical Tomotherapy unit (HiArt2).

Material and methods: Treatment plans for 15 prostate cancers, 5 head-neck tumours and 6 lung lesions were simulated with the Tomotherapy planning console. Similar parameters were chosen for the optimisation: a field width equal to 2.5 cm, a pitch of 0.3 and a modulation factor equal to 2 for prostate cases and 3 for head-neck and lung plans. An iterative least square inverse-planning optimisation process and a superposition/convolution dose calculation algorithm were implemented.

An investigation of dosimetrical accuracy was carried out upon the definition of an optimal treatment plan (i.e. good target volume coverage with sufficient sparing of critical structures): for each patient a comparison between measured and calculated dose distributions in homogeneous phantom was implemented, in both relative (film-EDR2) and absolute (ionisation chamber, Exradin A1SL 0.056 cc) ways. Absolute dose values, dose profiles, isodose curves and planar gamma function distributions (tolerance level:3%,3mm) were compared using the Analyze software implemented in the Tomotherapy planning station.

Results and discussion: Globally (89 points), the average agreement for punctual absolute dose is within 2.5%, considering both low and high dose gradient regions; the average absolute deviation is equal respectively to 2.5% (0.1%-17%) for prostate cases (49 points), 1.9% (0.7%-4.5%) for head-neck patients (16 points) and equal to 1.7% (0.1%-4.2%) for lung treatments (24 points). By considering only measured points within the target volume in low dose gradient regions, the % deviations were reduced respectively to 1.3% (0.1%-3.7%) for prostate cases, 1.5% (0.8%-2.5%) for head-neck plans and 0.9% (0.1%- 1.5%) for lung treatments. The same good results are obtained for planar dose distributions comparison: for dose regions between 100% and 50% of the prescribed dose, the disagreement between measured and calculated isodoses are within 2mm. In certain cases important differences were estimated for isodoses<30% of the prescribed dose, possibly correlated to film processing limits.

Conclusions: The results show good dosimetrical accuracy in homogeneous phantoms; subsequent measurements in non-homogenous media are also necessary to verify the acceptability of the dose calculation algorithm for critical conditions.

233

A new implant for automatic high precision real time patient positioning in radiotherapy (RT): a technical description of a GPS system for RT and on its initial test on a phantom and in man

B. Lennernas¹, R. Iustin², P. Albertsson¹, T. Gustafsson², S.

Nilsson³, S. Lewitt³, B. Rosengren²

¹Sahlgrenska University Hospital, Univ. of Gothenburg
Department of Oncology, Gothenburg Sweden

²Micropos Medical AB, Chalmers Innovation, Chalmers Univ.
of Technology, Gothenburg, Sweden

³University of Stockholm, Radiumhemmet, Stockholm,
Sweden

Purpose: To evaluate the precision of a new sensing technique and to evaluate the possibility for utilizing this technique for the precise positioning of patients and targets in radiation therapy (RT), specifically, Intensity Modulated Radiotherapy (IMRT)

Materials and methods: In the era of four dimensional RT (4DRT) and Intensity Modulated Radiotherapy (IMRT) it is essential to precisely detect and compensate for the movements of the target. Today, Electronic Portal Imaging (EPI) and Image Guided Radiotherapy (IGRT) are often used for patient and target movement detection. In this study the possibility of utilizing a new radio-wave based implant system (similar to the GPS) for patient positioning was tested. The system was tested in a phantom and on a human subject.

Results and conclusion: The system can automatically position the implant/ target/ patient more than 100 times per second with a resolution of 0,5 millimetres in X, Y and Z directions (max. error 2mm), throughout the entire RT chain

(from the initial CT to the last fraction of treatment). Rotation was not measured. Noise at a significant level was not detected in the clinic with the exception of that from an old and unshielded accelerator. In the human study and the first system prototype, the correlation obtained was 0.9 compared to the measured distance on the simulator X-ray image. Due to the high precision of this system, the planning target volume and dose to organs at risk conceivably could be substantially reduced. The system appears to be well adapted for automatic positioning in high precision radiotherapy.. Further human treatment studies are planned during 2005.

234

Cerenkov Light capture in optical fibres used for radiation therapy dosimetry

N. Suchowerska^{1,2}, S. Law¹, J. Lambert^{1,2}, D. McKenzie¹

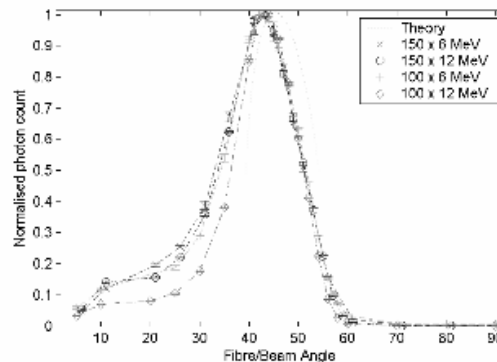
¹School of Physics, University of Sydney, Australia

²Royal Prince Alfred Hospital & University of Sydney,
Radiation Oncology, Sydney, Australia

³Australian Photonics CRC/Optical Fibre Technology Centre,
University of Sydney, Australia

Cerenkov light is generated in optical fibres when charged particles traveling faster than the local speed of light, traverse the fibre. The Cerenkov light is detected as a "noise" background on the signal being transmitted and introduces error into fibre optic dosimetry [DeBoer 1993]. Methods of eliminating or correcting for the Cerenkov background are a challenge in the design of accurate and reliable fibre optic dosimeters.

The conditions leading to the generation and coupling of Cerenkov light differ in teletherapy and brachytherapy. The generation of Cerenkov light in the fibre exposed to electron and photon megavoltage beams and in the vicinity of an Ir192 source of the type typically used in brachytherapy is simulated using Monte Carlo methods. The extent to which the Cerenkov light is captured as a propagating signal in the fibre depends on the angle between the fibre and the particle path. We have developed an analytical method for calculating the efficiency of capture, given the fibre and beam parameters.



We find good agreement between the predictions of our formalism and experimental results for typical teletherapy and brachytherapy configurations. There are two key findings significant to clinical dosimetry. First, the Cerenkov light received at the end of the fibre optic is sharply peaked at an angle of 40° between the beam and the fibre axis and that this peak is not symmetrical. Second, in a typical brachytherapy application the energy of the isotope emissions is largely below the Cerenkov threshold and the distribution in angles, leads to a weak coupling with propagating modes. These combined facts means that Cerenkov light is not a problem for clinical brachytherapy dosimetry.

De Boer SF, Beddar AS, Rawlinson JA. Optical filtering and spectral measurements of radiation-induced light in plastic scintillation dosimetry. *Physics in Medicine and Biology* [38] no.7:945-958, 1993

Lung

235

A prospective randomised controlled Phase II clinical trial to evaluate three immobilisation devices for intra-thoracic radiation therapy patients.

P. Browne, E. O'Shea, R. McCloy, A. Clayton-Lea, R. Murrells, M. Murphy, C. Booth, P. Thirion
St. Luke's Hospital, Dept of Radiation Oncology, Dublin, Ireland

Background: Accurate and reproducible patient immobilisation is essential for the delivery of high dose conformal radiation therapy for intra-thoracic cancer patients. However, the optimal immobilisation technique has yet to be determined. Currently in St. Luke's Hospital there is no specific immobilisation technique for the conformal treatment of patients with lung cancer.

Primary Objective: To evaluate the treatment set-up accuracy of three immobilisation techniques for conformal radiation therapy of intra-thoracic cancer.

Secondary Objectives:

- ◆ Patient satisfaction
- ◆ Cost-effectiveness and convenience of use

Methodology: This is a prospective randomised controlled Phase II clinical study. In this trial, 30 patients undergoing radical conformal radiotherapy for an intra-thoracic malignancy will be randomised to one of three immobilisation techniques that are available in St. Luke's Hospital – (A) headsponge plus kneefix, (B) breast board, and (C) lung board plus kneefix. 10 patients will be randomised to each treatment arm. The key features being investigated in the trial are accuracy of treatment technique and patient comfort.

Results & Conclusion: This trial opened for patient recruitment in March 2005 and is currently on-going. To date (April 2005) 6 patients have been randomised to this trial. Preliminary results will be available for presentation at the ESTRO conference in September 2005.

236

Impact of geometrical uncertainties on 3D-CRT and IMRT dose distributions for lung cancer treatment

M. Schwarz, J. van der Geer, M. van Herk, J. Lebesque, B. Mijnheer, E. Damen
The Netherlands Cancer Institute - Antoni van Leeuwenhoek Hospital, Radiation Oncology, Amsterdam, The Netherlands

Purpose: To quantify the effect of set-up errors and respiration motion on Conformal Radiotherapy (CRT) and IMRT dose distributions for non-small cell lung cancer (NSCLC) treatment.

Methods and materials: Irradiations of 5 NSCLC patients were planned with 3 techniques: CRT and IMRT1, both with homogeneous dose in the PTV, and IMRT2, where dose heterogeneity was allowed loosening the constraint on the maximum dose (Dmax). For each technique the PTV mean dose was set at the highest level compatible with the tolerance of the organs at risk (OARs) (lung, esophagus and spinal cord). Set-up errors were simulated for GTV and OARs, with a systematic (Σ) and random (σ) component of 1.3-1.5 mm and 2.0-3.1 mm (1SD). For the GTV, respiration was simulated as a periodic motion with a varying average position ($\Sigma, \sigma = 2$ mm). Four breathing scenarios were considered for the periodic breathing motion: 5 and 10 mm amplitude affecting either random error only (BS1 and BS2) or both systematic and random error (BS3 and BS4). For each patient and each scenario, 5000 treatment courses were simulated, producing probability distributions for the dosimetric parameters of interest, which were evaluated at the 95% probability level (PL).

Results: For CRT and IMRT1, all breathing scenarios except BS4 were associated with a small degradation of the GTV coverage (minimum dose (Dmin) reduction with respect to the static value ≤ 1.7 % at the 95% PL). Slightly increased effects of geometrical uncertainties were found for CRT and IMRT1 with BS4, and for IMRT2 for all scenarios except BS4

(decrease in GTV coverage for the 95% PL up to 5%). IMRT2 with BS4 showed the largest deterioration of the GTV dosimetric indices, reaching 7% for Dmin at the 95% PL. For all three techniques, removing the systematic error due to the periodic breathing motion was advantageous for a 10 mm respiration amplitude. Dmax in the spinal cord and the parameters predicting the risk of late esophageal toxicity were associated with a probability up to 50% of violating the dose tolerances.

Conclusions: Given the magnitude of set-up errors analyzed in this study, a 10 mm GTV-PTV margin is adequate for CRT and IMRT radiotherapy of NSCLC with an amplitude of the periodic breathing motion less than 10 mm. If the systematic error due to this type of motion is removed, a 10 mm margin will be adequate for all scenarios analyzed in our study. For some patients, defining a planning organ at risk volume for serial OARs is needed.

237

Positional stability of lung tumours during curative radiotherapy.

W. Sapru¹, T. Nøttrup¹, S. Korreman¹, L. Aarup¹, A.

Pedersen², H. Nystrøm¹, L. Specht², S. Månsson¹

¹Rigshospitalet 3994, Dept of Radiation Physics, Copenhagen, Denmark

²Rigshospitalet, Dept of oncology, Copenhagen, Denmark

Background: Lung cancer patients represent a growing population in Denmark. Recently, it has been documented that more patients can be cured by the combined use of surgery, chemotherapy and high-precision 3-dimensional radiotherapy. Planning radiotherapy of lung tumours is extremely challenging because the tumour changes position and the lung tissue changes density continuously due to respiration. Adequate irradiation requires that the tumour remains within the radiation field irrespective of its movement. Traditionally, this problem has been solved by the application of excessively large treatment fields, causing potentially toxic irradiation to healthy lung tissue.

Technique: A new innovative 4-dimensional technique, respiratory gating or breathing adapted radiotherapy (BART), can monitor the individual patient breathing and trigger beam-on during a discrete phase of each breathing cycle. This enables the radiation field margins to be reduced proportionally. A simple marker on the chest wall is used to monitor the movement of the chest wall. For lung tumours, however, the movement of the target is not always well correlated to the motion of the chest wall and the BART technique may be difficult to implement, since these patients may suffer from irregular breathing and changing breathing patterns over the course of treatment.

Patients and methods: 10 patients were included in the study. Breathing adapted CT-scans were acquired before, during and after the 30 fraction treatment for every patient. The commercially available Real-time Position Management-system™ was used to trigger scan-slice acquisition. For research purposes treatment plans with reduced margins were made on all the breathing adapted scans acquired before start of treatment.

The plans made on the initial breathing adapted CT scans were copied to the following scans with respect to optimal anatomical matching thus eliminating a potential set-up error.

Results: 10 patients were included, 1 patient was not scanned after treatment due to deterioration of health. In the 9 analysed patients the common pattern was high positional stability. For 8 patients the coverage of the tumour was sufficient with ITV margins of 0.5 cm in all dimensions. 1 patient had a weight lost of 11 kg during the treatment course and developed diffuse intrapulmonary infiltration impairing evaluation of target coverage. The ITV margin cannot be reduced further as there will always be motion due to heartbeat and the change in position over time. Evaluation of tumour shrinkage and migration will be presented.

Conclusion: Radiation oncologists taking up respiratory gating for lung cancer must consider margin reduction as a complex matter, not only influenced by intra breathing

variation in one breathing cycle. Further studies need to be carried out to evaluate the changes of tumour position over time.

238
Movement of tumour and mediastinal lymph nodes with respiration in patients with non small cell lung cancer (NSCLC)

S. Ahmad¹, J. McClelland³, A. Chandler⁴, J. Blackall³, S. Hughes¹, D. Hawkes³
¹Guy's & St Thomas' NHS Trust, Department of Radiotherapy, London, UK
³University College London, Centre for Medical Image Computing, London, UK
⁴King's College London, Division of Imaging Sciences, London, UK

Introduction: Patients receiving radical radiotherapy (RT) for NSCLC often have lymph nodes in the planning target volume (PTV). Lung tumours are known to move significantly during respiration. We have studied the movement of both mediastinal nodes and lung tumours in NSCLC patients to investigate the relationship of their motion trajectories.

Methods: CT scans were performed on 9 patients with NSCLC prior to starting radical RT. Two breath-hold images including both lungs and were acquired at inhale and exhale positions in the breathing cycle. An initial rigid registration between images was performed on the vertebral column to account for patient movement. A non-rigid registration followed to recover deformation between the extremes of breathing. The tumour and nodal areas were manually identified on the exhale image and mapped using the registration transformation onto the inhale image. Displacements in the superior-inferior, medial-lateral, and anterior-posterior directions were measured and the Euclidean displacement in millimetres was calculated as shown in the table along with the predominant direction(s) of movement.

Results

| Pt | SC | LH | RH | LP-T | RP-T | Tumour |
|----|--------|-------|-------|---------|------|--------|
| | mm | mm | mm | mm | mm | mm |
| 1 | 17 ↓ | 21 ↓ | 18 ↓ | 10 ↓ | 16 ↓ | 16 ↓ |
| 2 | 5 P | 4 ↑ | 3 P | 2 ↑ | 3 P | 2 P |
| 3 | 22 ↓/A | 23 ↓ | 18 ↓ | 14 ↓ | 16 ↓ | 31 ↓ |
| 4 | 4 A | 2 →/A | 4 A | 3 ↓/→ | 3 A | 4 A |
| 5 | 10 ↓/A | 8 A | 11 A | 8 A | 10 A | 10 A |
| 6 | 13 ↓/A | 15 ↓ | 16 A | 3 A | 13 A | 7 ↓ |
| 7 | 6 →/A | 7 ↓ | 6 →/A | 4 ↓/A | 7 A | 8 P |
| 8 | 9 ↓/→ | 10 ↓ | 15 A | 11 ← | 12 ← | 7 ↓ |
| 9 | 7 A | 9 ↓ | 5 ↓/A | 4 ↓/→/A | 4 A | 2 → |

Table key:

SC = Subcarinal nodes; **LH** = Left Hilar nodes; **RH** = Right Hilar nodes;
LP-T = Left Paratracheal nodes; **RP-T** = Right Paratracheal nodes;
 ↑ = Superior; ↓ = Inferior; → = Right; ← = Left; A = Anterior; P = Posterior

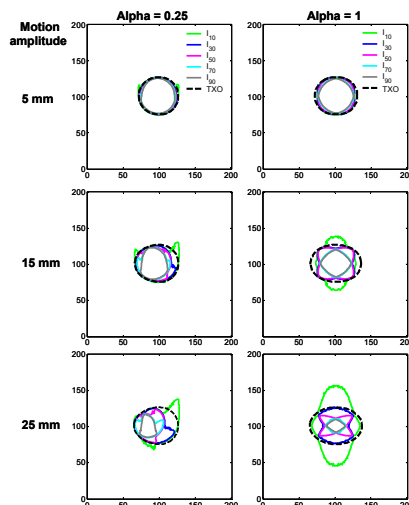
Conclusion: We have shown that there is significant respiratory motion both for tumours and mediastinal nodal groups and that its magnitude and direction varies substantially over the patient population as well as between anatomical sites. Importantly, we have observed that the nodal groups and tumours can move independently of each other. This has implications for PTV definition. These results suggest that adding the same margin to different parts of the PTV may be inadequate to account for respiration and that patient specific planning may be required to optimise RT treatment. The use of 4DCT patient specific motion models (as submitted by our group to this conference) may resolve some of the issues highlighted in this work.

239
The impact of lung tumor motion during CT image acquisition upon target delineation

I. Gagne¹, D. Robinson²
¹British Columbia Cancer Agency - Vancouver Island Centre, Department of Physics, Victoria, Canada
²Cross Cancer Institute, Department of Medical Physics, Edmonton, Canada

This study examined the ability of CT to accurately represent the total cross-section occupied (TXO) by a mobile target during image acquisition. Spheres with diameters of 10, 30 and 50 mm (all with a uniform density of 0.90 g/cm³) representing small, medium and large size lung tumors were simulated to move in a simple harmonic fashion, with various amplitudes and a 4 second period, in a homogeneous lung tissue background (density = 0.25 g/cm³) during image acquisition. A CT image reconstruction model developed in MATLAB [Version 6.5, Release 13, Mathworks Inc., June 2002] and experimentally validated under both static and dynamic conditions using high and low contrast geometries was used to generate the CT image of the mobile object and define the TXO. Three imaging techniques were examined and compared, a breath-hold scan, a typical rapid CT scan {1 second acquisition, alpha = 0.25} and a 'slow' CT scan {4 second acquisition, alpha = 1}. For each sphere/motion /scan combination, target contours spanning a wide range of static object contrasts above background [10:10:90%], were defined using a simple level threshold image segmentation technique. Target contours achieved with breath-hold CT scanning were virtually indistinguishable from one another and highly congruent with the TXO contour. For the full range of threshold levels and sphere sizes investigated, minimal spatial deviations (< 1 mm) between static contours and TXO contour were recorded. Target contours obtained with both rapid and 'slow' CT scanning were, on the other hand, divergent by varying degrees, from one another and from physically meaningful contours which might be associated with these mobile objects (see Figure 1 for example).

Two quantities, (1) TXO coverage and (2) unnecessary coverage, both expressed as a percentage of the TXO, were used to evaluate the impact of lung tumor motion on target delineation. In all cases examined, none of the dynamic contours fully encompassed the TXO. TXO coverage was found to decrease with increasing threshold level, increasing motion amplitude, decreasing sphere diameter and increasing acquisition time. Unnecessary coverage was prominent only at low threshold levels and ranged in values from a minimum of 0.6% to a maximum of 153%. The widespread failure of CT to accurately identify the TXO in dynamic situations results from the image degradation associated with the presence of motion-induced artifacts and not the simplicity of the delineation technique employed.



240

Systematic displacement of lung tumours during treatment: should we match on bone or on tumour?

*F. Van de Boomen, C. Hurkmans, K. Jaspers
Catharina Hospital, Radiation Oncology, Eindhoven, The Netherlands*

Introduction: A set-up correction protocol based on DRRs and EPIs is routinely used in our institution for lung cancer patients. This correction is based on matching of bony anatomy. However, this does not account for possible changes in the position of the tumour itself. We investigated the feasibility of using EPI for quantification and correction of tumour movement.

Methods and material: For 42 patients who underwent radical treatment of T1/2N0M0 lung cancer, orthogonal sets of EPIs were acquired for at least 6 treatment fractions. For the first group (n=32) a CCD camera-based EPID (Theraview, Cablon Medical) was used. A second group of patients (n=10) was imaged with an amorphous silicon (aSi) EPID (Iview, Elekta). EPIs and DRRs were matched independently by 3 observers based on bony anatomy and, separately, also based on the delineated tumour volume. Acquisition of EPIs took approximately 1-2 seconds, which is shorter than a breathing cycle. By averaging all the tumour matches per patient, the average tumour position could be determined. A separate analysis was performed on a subgroup of patients for which the inter-observer variation (IOV) of the tumour match was equal to the IOV of the bone match of the new aSi EPIDs.

Results: The 3D IOV for bone matches was significantly (p=0.0035) lower for the aSi-EPIs than for the camera-based EPIs.

For 23 out of the 32 patients from the camera-based EPID group and all 10 patients from the aSi EPID group a tumour match could be performed. The IOV for these tumour matches was comparable to the IOV for the camera-based bone matches. Only for 7 patients from the camera-based and 1 from the aSi group a tumour match in both directions was possible which met our criteria. This is 20% of all patients.

For this subgroup, the mean 3D tumour displacement relative to the planning CT was 4.5 mm. Especially in the ventro-dorsal and cranio-caudal direction large systematic displacements (around 4 mm) occurred.

Conclusion: Bone matches have a much smaller interobserver variation for aSi EPIs than for camera based EPIs. Only in a subgroup of 20% of the total population a reliable tumour match is possible. The tumour position during treatment, relative to the bony structures, can be systematically different from the planning position. Therefore, frequent tumour imaging during treatment is needed. However, EPIs are not suitable for this purpose.

Table 1: Set-up errors and interobserver variations for bone and tumour matches in mm.

| | | ML | CC | VD | 3D |
|--------------|----------------------------------|-----|------|------|-----|
| Bone match | Δ | 0.1 | -0.1 | 0.4 | |
| | Σ | 3.1 | 3.2 | 2.3 | 5.0 |
| | σ | 2.8 | 1.8 | 2 | 3.9 |
| | σ interobserver Camera | | | | 3.0 |
| | σ interobserver aSi | | | | 1.9 |
| Tumour match | Δ | 0.2 | 0.1 | -1.8 | |
| | Σ | 2.3 | 3.6 | 4.4 | 6.1 |
| | σ interobserver Camera | | | | 3.1 |
| | σ interobserver aSi | | | | 3.3 |
| | σ interobserver selection | | | | 1.9 |

241

Establishing baseline information for implementing ABC in thoracic radiation treatment

*E. O'Shea, F. McCabe, J. Armstrong, P. Thirion
St Lukes Hospital, Radiotherapy Department, Dublin, Ireland*

Background: Details regarding the breath-hold capabilities of the general thoracic radiotherapy patient population, whose tumour location and planning target volume is known to be affected by breathing motion, as opposed to highly selected patient groups with exceptionally good performance, are not available in the published literature. This research will establish if the reported feasible application of Active Breathing Control™ (ABC) is suitable for the more typical patients that are treated in a general radiotherapy department, particularly for lung cancer patients.

Aim: To establish baseline information essential for the clinical implementation of ABC – this includes determining the breath-holding capabilities of general thoracic (lung, breast and oesophagus) radiotherapy patients and the feasibility of using the ABC equipment including the identification of patient-specific and treatment technique characteristics that impact on the feasibility of using ABC and identifying necessary hardware and software modifications to the equipment.

Methodology: The duration of comfortable breath-hold and the number of breath-holds achieved by individual patients will be compared with the patient's treatment plan to determine the number of breath-holds hypothetically needed in order to deliver treatment under ABC conditions.

Results: 14 patients undergoing a radical course of thoracic radiotherapy have been recruited to date (April 2005) to this study. The procedure was well tolerated by 13 out of 14 patients. Specific data including the breath-hold duration, the ABC "threshold levels" and the number of breath-holds needed to receive a fraction of treatment will be available in Sept. 2005.

Conclusion: The number of breath-holds needed to deliver a treatment fraction was found to depend on both patient and treatment related characteristics: Treatment factors include treatment site, dose per fraction, number of fields, use of and type of wedge, dose rate of linear accelerator and use of portal imaging. Patient-specific characteristics identified to have an impact on tolerance of ABC include breathing difficulties, use of badly-fitting dentures, missing teeth, and high levels of stress/anxiety.

242

Heart complication following left-sided breast cancer radiotherapy: a gated CT study aiming to understand which patients might benefit from gated RT treatment.

B. Wennberg¹, M. Hussain², R. Odh², G. Gagliardi², B. Hedlund-Svedjemyr³, J. Bjöhle³, I. Lax², U. Lönn⁴, I. Näslund³, C. Svensson³

¹Karolinska Universitetssjukhuset, Medical Physics, Section of Radiation Therapy, Stockholm, Sweden

²Karolinska Universitetssjukhuset, Medical Physics, Stockholm, Sweden

³Karolinska Universitetssjukhuset, Oncology, Stockholm, Sweden

⁴Karolinska Universitetssjukhuset, Medical Physics and technology, Stockholm, Sweden

Purpose: to perform a gated CT study on left sided breast ca patients to create selection criteria for routine use of gated RT, aiming to decrease heart irradiation.

Methods and materials: the gating system used was the Varian real time positioning management system (RPM). This system uses a marker system placed on the chest or the abdomen of the patient. A PC-based system monitors the movements of the marker by a camera. The position of the marker can be used to trigger imaging or treatment. By using the 4DCT option (GE) combined with the RPM system we analyzed the impact of respiratory movements.

The study includes 20 patients. Patients were scanned in the treatment position. They were immobilized by using a wing-

board support for the arms and a high knee support. The patients were informed on how the system will use the breathing motions. No other coaching was done. The respiratory movements of the chest wall in the mamillary plane were measured and compared to the marker system; the maximum movements in the coronal and transverse direction were measured. For the heart the movements in the transverse plane were measured at the mamillary level and the maximum movement and the movement perpendicular to the (assumed) tangential fields were measured.

Results: Preliminary data shows a wide range of respiratory movements. The movements of the diaphragm ranging between 6.5 to 35 mm in the sagital plane and 8 to 49 mm in the coronal plane. And the hearts movements ranging from 3.5 to 13.0 mm in transversal plane, 6.5 to 24 mm in the sagital plane and in the coronal plane 3.7 to 16 mm. The selection of the marker system location on the patient turned out to be crucial. In fact, in order to obtain a detectable respiratory wave without affecting the natural respiration way of the patient, the markersystem was located on the abdomen instead than on the chestwall. To select patients that will have a benefit from gated treatments a gated CT-study has to be done – it is not possible from the outside to see if the hearts location associated with a higher risk of toxicity or if the motion of the heart from breathing is large enough to warrant gating procedures.

Conclusion: For every treatment type and fixations system a local study have to be done to evaluate the benefits of the gating system. For some left sided breast cancer patients gated treatment techniques to reduce the heart toxicity are warranted in our institution. A gated CT-study of the patient has to be done to see if hearts location is such that the gated technique is warranted.